



City Research Online

City, University of London Institutional Repository

Citation: Balasubramanian, V., de Boer, J., Feng, B., He, Y., Huang, M., Jejjala, V. and Naqvi, A. (2003). Multitrace superpotentials vs. matrix models. *Communications in Mathematical Physics*, 242, pp. 361-392. doi: 10.1007/s00220-003-0947-9

This is the unspecified version of the paper.

This version of the publication may differ from the final published version.

Permanent repository link: <https://openaccess.city.ac.uk/id/eprint/841/>

Link to published version: <http://dx.doi.org/10.1007/s00220-003-0947-9>

Copyright: City Research Online aims to make research outputs of City, University of London available to a wider audience. Copyright and Moral Rights remain with the author(s) and/or copyright holders. URLs from City Research Online may be freely distributed and linked to.

Reuse: Copies of full items can be used for personal research or study, educational, or not-for-profit purposes without prior permission or charge. Provided that the authors, title and full bibliographic details are credited, a hyperlink and/or URL is given for the original metadata page and the content is not changed in any way.

Multi-Trace Superpotentials vs. Matrix Models

Vijay Balasubramanian¹, Jan de Boer², Bo Feng³, Yang-Hui He¹, Min-xin Huang¹, Vishnu Jejjala⁴, and Asad Naqvi¹

1. David Rittenhouse Laboratories,
The University of Pennsylvania,
209 S. 33rd St., Philadelphia, PA 19104-6396

2. Institute of Theoretical Physics,
University of Amsterdam,
Valckenierstraat 65, 1018 XE,
Amsterdam, The Netherlands

3. Institute for Advanced Study,
Olden Lane, Princeton, NJ 08540

4. Institute for Particle Physics and Astrophysics
Department of Physics, Virginia Tech
Blacksburg, VA 24061

vijay@physics.upenn.edu, jdeboer@science.uva.nl, fengb@ias.edu, yanghe@physics.upenn.edu,
minxin@sas.upenn.edu, vishnu@vt.edu, naqvi@physics.upenn.edu

ABSTRACT: We consider $\mathcal{N} = 1$ supersymmetric $U(N)$ field theories in four dimensions with adjoint chiral matter and a multi-trace tree-level superpotential. We show that the computation of the effective action as a function of the glueball superfield localizes to computing matrix integrals. Unlike the single-trace case, holomorphy and symmetries do not forbid non-planar contributions. Nevertheless, only a special subset of the planar diagrams contributes to the exact result. Some of the data of this subset can be computed from the large- N limit of an associated multi-trace Matrix model. However, the prescription *differs* in important respects from that of Dijkgraaf and Vafa for single-trace superpotentials in that the field theory effective action is *not* the derivative of a multi-trace matrix model free energy. The basic subtlety involves the correct identification of the field theory glueball as a variable in the Matrix model, as we show via an auxiliary construction involving a single-trace matrix model with additional singlet fields which are integrated out to compute the multi-trace results. Along the way we also describe a general technique for computing the large- N limits of multi-trace Matrix models and raise the challenge of finding the field theories whose effective actions they may compute. Since our models can be treated as $\mathcal{N} = 1$ deformations of pure $\mathcal{N} = 2$ gauge theory, we show that the effective superpotential that we compute also follows from the $\mathcal{N} = 2$ Seiberg-Witten solution. Finally, we observe an interesting connection between multi-trace local theories and non-local field theory.

KEYWORDS: Matrix Models, N=1 Supersymmetric Gauge Theory, Superpotentials, Multi-Trace.

Contents

1. Introduction	1
2. Multi-Trace Superpotentials from Perturbation Theory	4
2.1 A Schematic Review of the Field Theory Superpotential Computation	4
2.2 Computation of a Multi-Trace Superpotential	8
2.3 Which Diagrams Contribute: Selection Rules	11
2.4 Summing Pasted Diagrams	13
2.5 Perturbative Calculation	15
2.5.1 First Order	15
2.5.2 Second Order	15
2.5.3 Third Order	16
2.5.4 Obtaining the Effective Action	16
2.6 Multiple Traces, Pasted Diagrams and Nonlocality	18
3. The Field Theory Analysis	18
3.1 The Classical Vacua	19
3.2 The Exact Superpotential in the Confining Vacuum	20
3.3 An Explicit Example	22
4. The Matrix Model	23
4.1 The Mean-Field Method	23
4.2 Generalized Multi-Trace Deformations	25
5. Linearizing Traces: How To Identify the Glueball?	27
5.1 Field Theory Computation of $\mathbf{W}_{\text{single}}(\mathbf{A}, \mathbf{S})$ and Pasted Matrix Diagrams	27
5.2 Matrix model perspective	29
5.3 General Multi-trace Operators	30
6. Conclusion	31

1. Introduction

Dijkgraaf and Vafa have recently made the remarkable proposal that the superpotential and other holomorphic data of $\mathcal{N} = 1$ supersymmetric gauge theories in four dimensions can be computed from an auxiliary Matrix model [1, 2, 3]. While the original proposal arose from consideration

of stringy dualities arising in context of geometrically engineered field theories, two recent papers have suggested direct field theory proofs of the proposal [4, 5]. These works considered $U(N)$ gauge theories with an adjoint chiral matter multiplet Φ and a tree-level superpotential $W(\Phi) = \sum_k g_k \text{Tr}(\Phi^k)$. Using somewhat different techniques ([4] uses properties of superspace perturbation theory while [5] relies on factorization of chiral correlation functions, symmetries, and the Konishi anomaly) these papers conclude that:

1. The computation of the effective superpotential as a function of the glueball superfield reduces to computing matrix integrals.
2. Because of holomorphy and symmetries (or properties of superspace perturbation theory), only planar Feynman diagrams contribute.
3. These diagrams can be summed up by the large- N limit of an auxiliary Matrix model. The field theory effective action is obtained as a derivative of the Matrix model free energy.

Various generalizations and extensions of these ideas (*e.g.*, $\mathcal{N} = 1^*$ theories [6, 7], fundamental matter [8, 9], quantum moduli spaces [10], non-supersymmetric cases [11], other gauge groups [12, 13, 14, 15], baryonic matter [16, 17], gravitational corrections [18, 19], and Seiberg Duality [20, 21]) have been considered in the recent literature.

A stringent and simple test of the Dijkgraaf-Vafa proposal and of the proofs presented in [4, 5] is to consider superpotentials containing multi-trace terms such as

$$W(\Phi) = g_2 \text{Tr}(\Phi^2) + g_4 \text{Tr}(\Phi^4) + \tilde{g}_2 (\text{Tr}(\Phi^2))^2. \quad (1.1)$$

We will show that for such multi-trace theories:

1. The computation of the effective superpotential as a function of the glueball superfield still reduces to computing matrix integrals.
2. Holomorphy and symmetries do not forbid non-planar contributions; nevertheless only a certain subset of the planar diagrams contributes to the effective superpotential.
3. This subclass of planar graphs also contributes to the large- N limit of an associated multi-trace Matrix model. However, because of differences in combinatorial factors, the field theory effective superpotential *cannot* be obtained simply as a derivative of the multi-trace Matrix model free energy as in [3].
4. Multi-trace theories can be linearized in traces by the addition of auxiliary singlet fields A_i . The superpotentials for these theories as a function of both the A_i and the glueball can be computed from an associated Matrix model. This shows that the basic subtlety involves the correct identification of the field theory glueball as a variable in a related Matrix model.

The plan of this paper is as follows. In Sec. 2 we carefully analyze the methods of [4] and generalize them so that they apply to an $\mathcal{N} = 1$ $U(N)$ gauge theory in four dimensions with a tree-level superpotential of the form (1.1). Along the way we introduce some new techniques that deepen

our understanding of the selection rules determining which perturbative field theory diagrams contribute to the effective superpotential of an $\mathcal{N} = 1$ field theory. Using this understanding we demonstrate how the conclusions (1) and (2) above arise and show that contributing diagrams are tree-like graphs in which single-trace diagrams are pasted together by double-trace vertices through which no momentum flows. We illustrate our results by explicitly computing the superpotential to the first few orders in perturbation theory. Finally, we observe an intriguing connection between multi-trace local theories and non-local field theory.

Since the field content of pure $\mathcal{N} = 2$ supersymmetric $U(N)$ gauge theory in four dimensions consists in $\mathcal{N} = 1$ language of a vector multiplet \mathcal{W}_α and an adjoint chiral multiplet Φ , the superpotential (1.1) can be treated as a deformation of an $\mathcal{N} = 2$ theory to an $\mathcal{N} = 1$ theory. Hence, we can use global symmetries, holomorphy, regularity conditions, and the Seiberg-Witten solution of $\mathcal{N} = 2$ gauge theory to compute the exact superpotential. We carry out this procedure in Sec. 3, using the fact that the vacuum expectation value of the product of chiral operators $\langle \text{Tr}(\Phi^2)^2 \rangle$ factorizes as $\langle \text{Tr}(\Phi^2) \rangle^2$. We show that the result exactly captures the subset of the planar diagrams that contribute to the exact field theory superpotential. The assumption of factorization in the Seiberg-Witten analysis is equivalent to the vanishing of a certain subset of planar diagrams in our perturbative computations.

In Sec. 4 we demonstrate a general technique for solving $U(M)$ matrix models (or general complex matrix models) with multi-trace potentials. The essential observation, following Das, Dhar, Sengupta, and Wadia [22], is that in the large- M limit, mean field methods can be used to solve for the effect on a single matrix eigenvalue of the rest of the matrix. We explain the general method and solve two examples in detail. The first example has a potential $V(\Phi) = M(g_2 \text{Tr}(\Phi^2) + g_4 \text{Tr}(\Phi^4) + \frac{\tilde{g}_2}{M} \text{Tr}(\Phi^2)^2)$ for $\phi \in U(M)$. By expanding the exact large- M result in powers of the couplings we demonstrate how this limit computes the data relevant for a certain subset of the planar contributions to the effective action of the field theory with the tree-level superpotential in (1.1). In the proposal of Dijkgraaf and Vafa [3] and the subsequent generalizations (*e.g.*, [6] to [21]), the field theory effective action was related simply to the free energies of auxiliary matrix models and their derivatives. We demonstrate the absence of such a relation between multi-trace field theories and multi-trace Matrix models. As a further illustration of the mean field technique for computing large- M limits, we study a matrix model with a general quartic potential.

Multi-trace field theories can be linearized in traces by the introduction of new singlet fields which can be integrated out to produce the multi-trace theory. In Sec. 5 we show how this procedure is carried out and relate the resulting linearized superpotential to a Matrix model following the techniques of [4]. In the Matrix model integrating out the singlets at the level of the free energy reproduces the multi-trace results that do not agree with the field theory. However, integrating out after computing the linearized field theory superpotential leads to agreement. This shows that the basic subtlety here involves the correct identification of the field theory glueball as a variable in an associated Matrix model.

It is worth mentioning several further reasons why multi-trace superpotentials are interesting. First of all, the general deformation of a pure $\mathcal{N} = 2$ field theory to an $\mathcal{N} = 1$ theory with ad-

joint matter involves multi-trace superpotentials, and therefore these deformations are important to understand. What is more, multi-trace superpotentials cannot be geometrically engineered [23] in the usual manner for a simple reason: in geometric engineering of gauge theories the tree-level superpotential arises from a disc diagram for open strings on a D-brane and these, having only one boundary, produce single-trace terms. In this context, even if multi-trace terms could be produced by quantum corrections, their coefficients would be determined by the tree-level couplings and would not be freely tunable. Hence comparison of the low-energy physics arising from multi-trace superpotentials with the corresponding Matrix model calculations is a useful probe of the extent to which the Dijkgraaf-Vafa proposal is tied to its geometric and D-brane origins. In addition to these motivations, it is worth recalling that the double scaling limit of the $U(N)$ matrix model with a double-trace potential is related to a theory of two-dimensional gravity with a cosmological constant. This matrix model also displays phase transitions between smooth, branched polymer and intermediate phases [22]. It would be interesting to understand whether and how these phenomena manifest themselves as effects in a four dimensional field theory. The results of our paper suggest that these phase transitions and the physics of two-dimensional cosmological constants are embedded within four-dimensional field theory. It would be interesting to explore this. Finally, multi-trace deformations of field theories have recently made an appearance in the contexts of the *AdS/CFT* correspondence and a proposed definition of string theories with a nonlocal worldsheet theory [24].

2. Multi-Trace Superpotentials from Perturbation Theory

In this section we begin by reviewing the field theoretic proof that when treated as a function of the glueball superfield, the effective superpotential of an $\mathcal{N} = 1$ supersymmetric gauge theory with single-trace tree-level interactions is computed by planar matrix diagrams [4, 5]. We will then describe how these arguments are modified by the presence of multi-trace terms in the tree-level action. Finally, we will explicitly illustrate our reasoning by perturbatively computing the diagrams that contribute to the effective superpotential of a multi-trace theory up to third order in the couplings. We will always work around a vacuum with unbroken $U(N)$ symmetry.

2.1 A Schematic Review of the Field Theory Superpotential Computation

Below we give a schematic description of the methods of [4] for the computation of the effective superpotential of an $\mathcal{N} = 1$ field theory. While [4] discussed theories with single-trace Lagrangians, we will find that most of their arguments will generalize easily to multi-trace theories.

1. The Action: The matter action for an $\mathcal{N} = 1$ $U(N)$ gauge theory with a vector multiplet V , a massive chiral superfield Φ , and superpotential $W(\Phi)$, is given in superspace by

$$S(\Phi, \bar{\Phi}) = \int d^4x d^4\theta \bar{\Phi} e^V \Phi + \int d^4x d^2\theta W(\Phi) + \text{h.c.} \quad (2.1)$$

2. The Goal: We seek to compute the effective superpotential as a function of the glueball superfield

$$S = \frac{1}{32\pi^2} \text{Tr}(\mathcal{W}^\alpha \mathcal{W}_\alpha), \quad (2.2)$$

where

$$\mathcal{W}_\alpha = i\overline{D}^2 e^{-V} D_\alpha e^V \quad (2.3)$$

is the gauge field strength of V , with $D_\alpha = \partial/\partial\theta^\alpha$ and $\overline{D}_{\dot{\alpha}} = \partial/\partial\bar{\theta}^{\dot{\alpha}} + i\theta^\alpha\partial_{\alpha\dot{\alpha}}$ the superspace covariant derivatives, and $D^2 = \frac{1}{2}D^\alpha D_\alpha$ and $\overline{D}^2 = \frac{1}{2}\overline{D}^{\dot{\alpha}}\overline{D}_{\dot{\alpha}}$. The gluino condensate S is a commuting field constructed out of a pair of fermionic operators \mathcal{W}_α .

3. The Power of Holomorphy: We are interested in expressing the effective superpotential in terms of the *chiral* glueball superfield S . Holomorphy tells us that it will be independent of the parameters of the anti-holomorphic part of the tree-level superpotential. Therefore, without loss of generality, we can choose a particularly simple form for $\overline{W}(\overline{\Phi})$:

$$\overline{W}(\overline{\Phi}) = \frac{1}{2}\overline{m}\overline{\Phi}^2. \quad (2.4)$$

Integrating out the anti-holomorphic fields and performing standard superspace manipulations as discussed in Sec. 2 of [4], gives

$$S = \int d^4x d^2\theta \left(-\frac{1}{2\overline{m}}\Phi(\square - i\mathcal{W}^\alpha D_\alpha)\Phi + W_{tree}(\Phi) \right) \quad (2.5)$$

as the part of the action that is relevant for computing the effective potential as a function of S . Here, $\square = \frac{1}{2}\partial_{\alpha\dot{\alpha}}\partial^{\alpha\dot{\alpha}}$ is the d'Alembertian, and W_{tree} is the tree-level superpotential, expanded as $\frac{1}{2}m\Phi^2 + \text{interactions}$. (The reader may consult Sec. 2 of [4] for a discussion of various subtleties such as why the \square can be taken as the ordinary d'Alembertian as opposed to a gauge covariantized \square_{cov}).

4. The Propagator: After reduction into the form (2.5), the quadratic part gives the propagator. We write the covariant derivative in terms of Grassmann momentum variables

$$D_\alpha = \partial/\partial\theta^\alpha := -i\pi_\alpha, \quad (2.6)$$

and it has been shown in [4] that by rescaling the momenta we can put $\overline{m} = 1$ since all \overline{m} dependence cancels out. Then the momentum space representation of the propagator is simply

$$\int_0^\infty ds_i \exp(-s_i(p_i^2 + \mathcal{W}^\alpha \pi_{i\alpha} + m)), \quad (2.7)$$

where s_i is the Schwinger time parameter of i -th Feynman propagator. Here the precise form of the $\mathcal{W}^\alpha \pi_\alpha$ depends on the representation of the gauge group that is carried by the field propagating in the loop.

5. Calculation of Feynman Diagrams: The effective superpotential as a function of the glueball S is a sum of vacuum Feynman diagrams computed in the background of a fixed constant \mathcal{W}_α leading to insertions of this field along propagators. In general there will be ℓ momentum loops, and the corresponding momenta must be integrated over yielding the contribution

$$I = \left(\int \prod_{a,i} d^4 p_a ds_i e^{-s_i p_i^2} \right) \cdot \left(\int \prod_{a,i} d^2 \pi_a ds_i e^{-s_i \mathcal{W}^\alpha \pi_{i\alpha}} \right) \cdot \left(\int \prod_i ds_i e^{-s_i m} \right) \\ = I_{boson} \cdot I_{fermion} \cdot \frac{1}{m^P} \quad (2.8)$$

to the overall amplitude. Here a labels momentum loops, while $i = 1, \dots, P$ labels propagators. The momenta in the propagators are linear combinations of the loop momenta because of momentum conservation.

6. Bosonic Momentum Integrations: The bosonic contribution can be expressed as

$$I_{boson} = \int \prod_{a=1}^{\ell} \frac{d^4 p_a}{(2\pi)^4} \exp \left[- \sum_{a,b} p_a M_{ab}(s) p_b \right] = \frac{1}{(4\pi)^{2\ell}} \frac{1}{(\det M(s))^2}, \quad (2.9)$$

where we have defined the momentum of the i -th propagator in terms of the independent loop momenta p_a

$$p_i = \sum_a L_{ia} p_a \quad (2.10)$$

via the matrix elements $L_{ia} \in \{0, \pm 1\}$ and

$$M_{ab}(s) = \sum_i s_i L_{ia} L_{ib}. \quad (2.11)$$

7. Which Diagrams Contribute: Since each momentum loop comes with two fermionic π_α integrations (2.8) a non-zero amplitude will require the insertion of 2ℓ π_α s. From (2.7) we see that that π_α insertions arise from the power series expansion of the fermionic part of the propagator and that each π_α is accompanied by a \mathcal{W}_α . So in total we expect an amplitude containing 2ℓ factors of \mathcal{W}_α . Furthermore, since we wish to compute the superpotential as a function of $S \sim \text{Tr}(\mathcal{W}^\alpha \mathcal{W}_\alpha)$ each index loop can only have zero or two \mathcal{W}_α insertions. These considerations together imply that if a diagram contributes to the effective superpotential as function of the S , then number of index loops h must be greater than or equal to the number of momentum loops ℓ , *i.e.*,

$$h \geq \ell. \quad (2.12)$$

8. Planarity: The above considerations are completely general. Now let us specialize to $U(N)$ theories with single-trace operators. A diagram with ℓ momentum loops has

$$h = \ell + 1 - 2g \quad (2.13)$$

index loops, where g is the genus of the surface generated by 't Hooft double line notation. Combining this with (2.12) tell us that $g = 0$, *i.e.*, only planar diagrams contribute.

9. Doing The Fermionic Integrations: First let us discuss the combinatorial factors that arise from the fermionic integrations. Since the number of momentum loops is one less than the number of index loops, we must choose which of the latter to leave free of \mathcal{W}_α insertions. This gives a combinatorial factor of h , and the empty index loop gives a factor of N from the sum over color. For each loop with two \mathcal{W}_α insertions we get a factor of $\frac{1}{2}\mathcal{W}^\alpha\mathcal{W}_\alpha = 16\pi^2S$. Since we are dealing with adjoint matter, the action of \mathcal{W}_α is through a commutator

$$\exp(-s_i[\mathcal{W}_i^\alpha, -]\pi_{i\alpha}) \quad (2.14)$$

in the Schwinger term. (See the appendix of [12] for a nice explanation of this notation as it appears in [4]. In Sec. 2.2 we will give an alternative discussion of the fermionic integrations that clarifies various points.) As in the bosonic integrals above, it is convenient to express the fermionic propagator momenta as sums of the independent loop momenta:

$$\pi_{i\alpha} = \sum_a L_{ia} \pi_{a\alpha}, \quad (2.15)$$

where the L_{ia} are the same matrix elements as introduced above. The authors of [4] also find it convenient to introduce auxiliary fermionic variables via the equation

$$\mathcal{W}_i^\alpha = \sum_a L_{ia} \mathcal{W}_a^\alpha. \quad (2.16)$$

Here, the $L_{ia} = \pm 1$ denotes the left- or right-action of the commutator. In terms of the \mathcal{W}_a^α , the fermionic contribution to the amplitude can be written as

$$\begin{aligned} I_{fermion} &= Nh(16\pi^2S)^\ell \int \prod_a d^2\pi_a d^2\mathcal{W}_a \exp \left[- \sum_{a,b} \mathcal{W}_a^\alpha M_{ab}(s) \pi_{b\alpha} \right] \\ &= (4\pi)^{2\ell} NhS^\ell (\det M(s))^2. \end{aligned} \quad (2.17)$$

10. Localization: The Schwinger parameter dependence in the bosonic and fermionic momentum integrations cancel exactly

$$I_{boson} \cdot I_{fermion} = NhS^\ell, \quad (2.18)$$

implying that the computation of the effective superpotential as a function of the S localizes to summing matrix integrals. All the four-dimensional spacetime dependence has washed out. The full effective superpotential $W_{eff}(S)$ is thus a sum over planar matrix graphs with the addition of the Veneziano-Yankielowicz term for the pure Yang-Mills theory [25]. The terms in the effective action proportional to S^ℓ arise exclusively from planar graphs with ℓ momentum loops giving a perturbative computation of the *exact* superpotential.

11. The Matrix Model: The localization of the field theory computation to a set of planar matrix diagrams suggests that the sum of diagrams can be computed exactly by the large- M

limit of a bosonic Matrix model. (We distinguish between M , the rank of the matrices in the Matrix model and N , the rank of the gauge group.) The prescription of Dijkgraaf and Vafa does exactly this for single-trace superpotentials. Since the number of momentum loops is one less than the number of index loops in a planar diagram, the net result of the bosonic and fermionic integrations in (2.18) can be written as

$$I_{boson} \cdot I_{fermion} = N \frac{\partial S^h}{\partial S}. \quad (2.19)$$

Because of this, the perturbative part of the effective superpotential, namely the sum over planar diagrams in the field theory, can be written in terms of the genus zero free energy $\mathcal{F}_0(S)$ of the corresponding matrix model:

$$W_{pert}(S) = N \frac{\partial}{\partial S} \mathcal{F}_0(S), \quad (2.20)$$

$$\mathcal{F}_0(S) = \sum_h \mathcal{F}_{0,h} S^h. \quad (2.21)$$

This free energy is conveniently isolated by taking the large- M limit of the zero-dimensional one-matrix model with $M \times M$ matrices¹ Φ and potential $W(\Phi)$ whose partition function is given by

$$Z = \exp(M^2 \mathcal{F}_0) = \frac{1}{\text{Vol}(U(M))} \int [D\Phi] \exp\left(-\frac{1}{g_s} \text{Tr} W(\Phi)\right). \quad (2.22)$$

In this matrix model every index loop gives a power of M just as in the field theory computation, and all but one index loop gives a power of S . Because of this simple fact the powers of the gluino condensate in the field theory superpotential can be conveniently counted by identifying it with the 't Hooft coupling $S \equiv M g_s$, and then differentiating the matrix model free energy as in (2.20). Rather surprisingly the Veneziano-Yankielowicz term in $W_{eff}(S)$ arises from the volume factor in the integration over matrices in (2.22).

One important unanswered question is why the low-energy dynamics simplifies so much when written in terms of the gluino condensates.

2.2 Computation of a Multi-Trace Superpotential

We have reviewed above how the field theory calculation of the effective superpotential for a single-trace theory localizes to a matrix model computation. In this subsection we show how the argument is modified when the tree-level superpotential includes multi-trace terms. We consider an $\mathcal{N} = 1$ theory with the tree-level superpotential

$$W_{tree} = \frac{1}{2} \text{Tr}(\Phi^2) + g_4 \text{Tr}(\Phi^4) + \tilde{g}_2 (\text{Tr}(\Phi^2))^2. \quad (2.23)$$

¹The original papers of Dijkgraaf and Vafa [1, 2] consider $M \times M$ Hermitian matrices (*i.e.* matrices with real eigenvalues λ_i). In fact, we should think of the matrices as belonging to $GL(M, \mathbb{C})$ with eigenvalues distributed along contours in the complex plane rather than along domains on the real axis. The prior results do not depend crucially on this point. Indeed, they carry through exactly by analytic continuation. We thank David Berenstein for emphasizing this to us.

To set the stage for our perturbative computation of the effective superpotential we begin by analyzing the structure of the new diagrams introduced by the double-trace term. If $\tilde{g}_2 = 0$, the connected diagrams we get are the familiar single-trace ones; we will call these *primitive diagrams*. When $\tilde{g}_2 \neq 0$ propagators in primitive diagrams can be spliced together by new double-trace vertices. It is useful to do an explicit example to see how this splicing occurs. As an example, let

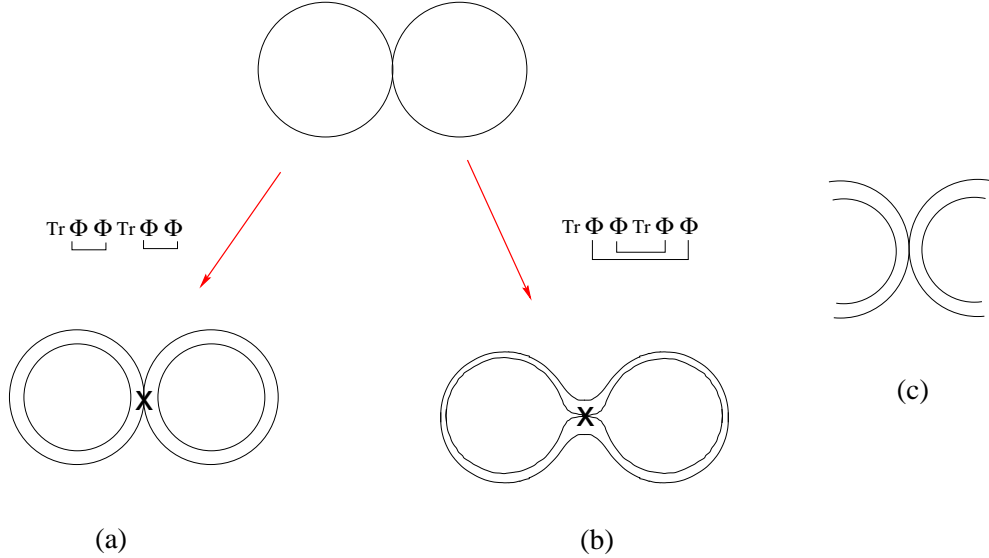


Figure 1: Two ways in which the double-trace operator: $\text{Tr}(\Phi^2)\text{Tr}(\Phi^2)$ can be contracted using the vertex shown in (c).

us study the expectation value of the double-trace operator: $\langle \text{Tr}(\Phi^2)\text{Tr}(\Phi^2) \rangle$. To lowest order in couplings, the two ways to contract Φ s give rise to the two diagrams in Figure 1. When we draw these diagrams in double line notation, we find that Figure 1a corresponding to $\text{Tr}(\overline{\Phi\Phi})\text{Tr}(\overline{\Phi\Phi})$ has four index loops, while Figure 1b corresponding to $\text{Tr}(\overline{\Phi\Phi})\text{Tr}(\overline{\Phi\Phi})$ has only two index loops. Both these graphs have two momentum loops. For our purposes both of these Feynman diagrams can also be generated by a simple pictorial algorithm: we splice together propagators of primitive diagrams using the vertex in Figure 1c, as displayed in Figure 2a and b. All graphs of the double-trace theory can be generated from primitive diagrams by this simple algorithm. Note that the number of index loops never changes when primitive diagrams are spliced by this pictorial algorithm.

If a splicing of diagrams does not create a new momentum loop we say that the diagrams have been *pasted* together. This happens when the diagrams being spliced are originally disconnected as, for example, in Figure 2a. In fact because of momentum conservation, no momentum at all flows between pasted diagrams. If a new momentum loop is created we say that that the diagrams have been *pinched*. This happens when two propagators within an already connected diagram are spliced together as, for example, in Figure 2b. In this example one momentum loop becomes two because momentum can flow through the double-trace vertex. Further examples of pinched diagrams are given in Figure 3 where the new loop arises from momentum flowing between the primitive diagrams via double-trace vertices.

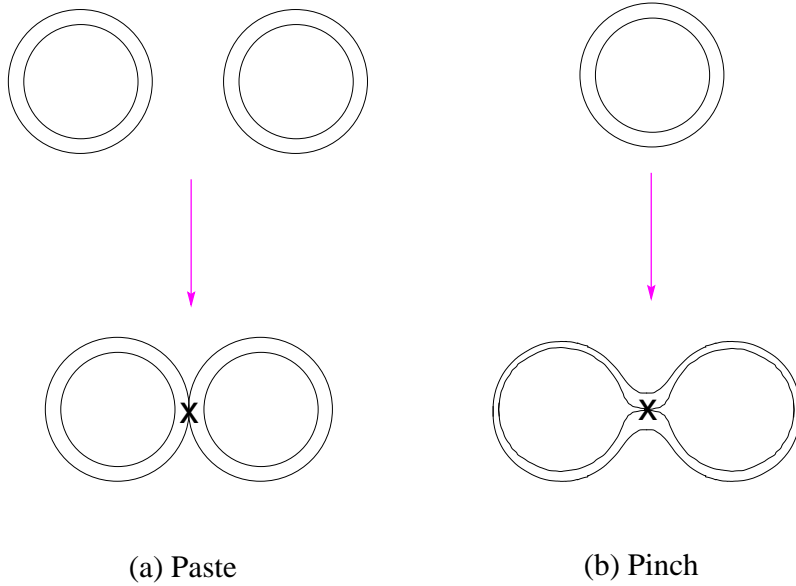


Figure 2: With the inclusion of the double-trace term we need new types of vertices. These can be obtained from the “primitive” diagrams associated with the pure single-trace superpotential by (a) pasting or (b) pinching. The vertices have been marked with a cross.

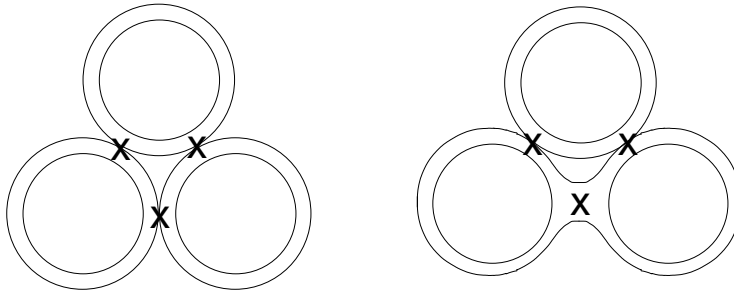


Figure 3: More examples of “pinched” diagrams.

To make the above statement more clear, let us provide some calculations. First, according to our operation, the number of double index loops never increases whether under pasting or pinching. Second, we can calculate the total number of independent momentum loops ℓ by $\ell = P - V + 1$ where P is the number of propagators and V , the number of vertices. If we connect two separate diagrams by *pasting*, we will have $P_{tot} = (P_1 - 1) + (P_2 - 1) + 4$, $V_{tot} = V_1 + V_2 + 1$ and

$$\ell_{tot} = P_{tot} - V_{tot} + 1 = \ell_1 + \ell_2, \quad (2.24)$$

which means that the total number of momentum loops is just the sum of the individual ones. If we insert the double-trace vertex in a single connected diagram by *pinching*, we will have $P_{tot} = P - 2 + 4$, $V_{tot} = V + 1$, and

$$\ell_{tot} = P_{tot} - V_{tot} + 1 = \ell + 1, \quad (2.25)$$

which indicates the creation of one new momentum loop.

Having understood the structure of double-trace diagrams in this way, we can adapt the techniques of [4] to our case. The steps 1-6 as described in Sec. 2.1 go through without modification since they are independent of the details of the tree-level superpotential. However the steps 7-11 are modified in various ways. First of all naive counting of powers of fermionic momenta as in step 7 leads to the selection rule

$$h \geq \ell, \tag{2.26}$$

where h is the total number of index loops and ℓ is the total number of momentum loops. (The holomorphy and symmetry based arguments of [5] would lead to the same conclusion.) Since no momentum flows between pasted primitive diagrams it is clear that this selection rule would permit some of the primitive components to be non-planar. Likewise, both planar and some non-planar pinching diagrams are admitted. An example of a planar pinching diagram that can contribute according to this rule is Figure 2b. However, we will show in the next subsection that more careful consideration of the structure of perturbative diagrams shows that only diagrams built by pasting planar primitive graphs give non-zero contributions to the effective superpotential.

2.3 Which Diagrams Contribute: Selection Rules

In order to explain which diagrams give non-zero contributions to the multi-trace superpotential it is useful to first give another perspective on the fermionic momentum integrations described in steps 7–9 above. A key step in the argument of [4] was to split the glueball insertions up in terms of auxiliary fermionic variables associated with each of the momentum loops as in (2.16). We will take a somewhat different approach. In the end we want to attach zero or two fields $\mathcal{W}_{(p)}^\alpha$ to each *index* loop, where p labels the index loop, and the total number of such fields must bring down enough fermionic momenta to soak up the corresponding integrations. On each oriented propagator, with momentum $\pi_{i\alpha}$, we have a left index line which we label p_L and a right index line which we label p_R . Because of the commutator in (2.14), the contribution of this propagator will be

$$\exp(-s_i(\pi_{i\alpha}(\mathcal{W}_{(p_L)}^\alpha - \mathcal{W}_{(p_R)}^\alpha))). \tag{2.27}$$

Notice that we are omitting $U(N)$ indices, which are simply replaced by the different index loop labels. In a standard planar diagram for a single-trace theory, we have one more index loop than momentum loop. So even in this case the choice of auxiliary variables in (2.27) is not quite the same as in (2.16), since the number of \mathcal{W}_α s is twice the number of index loops in (2.27) while the number of auxiliary variables is twice the number of momentum loops in (2.16).

Now in order to soak up the fermionic π integrations in (2.8), we must expand (2.27) in powers and extract terms of the form

$$\mathcal{W}_{(p_1)}^2 \mathcal{W}_{(p_2)}^2 \dots \mathcal{W}_{(p_\ell)}^2, \tag{2.28}$$

where ℓ is the number of momentum loops and all the p_i are distinct. The range of p is over $1, \dots, h$, with h the number of index loops. In the integral over the anticommuting momenta, we have all h $\mathcal{W}_{(p)}$ appearing. However, one linear combination, which is the ‘center of mass’ of the $\mathcal{W}_{(p)}$, does not appear. This can be seen from (2.27): if we add a constant to all $\mathcal{W}_{(p)}$ simultaneously, the

propagators do not change. Thus, without loss of generality, one can set the $\mathcal{W}_{(p)}$ corresponding to the outer loop in a planar diagram equal to zero. Let us assume this variable is $\mathcal{W}_{(h)}$ and later reinstate it. All $\mathcal{W}_{(p)}$ corresponding to inner index loops remain, leaving as many of these as there are momentum loops in a planar diagram. It is then straightforward to demonstrate that the \mathcal{W} appearing in (2.16) in linear combinations reproduce the relations between propagator momenta and loop momenta. In other words, in this ‘‘gauge’’ where the \mathcal{W} corresponding to the outer loop is zero, we recover the decomposition of \mathcal{W}_α in terms of auxiliary fermions associated to momentum loops that was used in [4] and reviewed in (2.16) above.

We can now reproduce the overall factors arising from the fermionic integrations in the planar diagrams contributing to (2.17). The result from the π integrations is some constant times

$$\prod_{p=1}^{\ell} \mathcal{W}_{(p)}^2. \quad (2.29)$$

Reinstating $\mathcal{W}_{(h)}$ by undoing the gauge choice, namely by shifting

$$\mathcal{W}_{(p)} \rightarrow \mathcal{W}_{(p)} + \mathcal{W}_{(h)} \quad (2.30)$$

for $p = 1, \dots, h - 1$, (2.29) becomes

$$\prod_{p=1}^{\ell} (\mathcal{W}_{(p)} + \mathcal{W}_{(h)})^2. \quad (2.31)$$

The terms on which each index loop there has either zero or two \mathcal{W} insertions are easily extracted:

$$\sum_{k=1}^h \left(\prod_{p \neq k} \mathcal{W}_{(p)}^2 \right). \quad (2.32)$$

In this final result we should replace each of the $\mathcal{W}_{(p)}^2$ by S , and therefore the final result is of the form

$$hS^{h-1}, \quad (2.33)$$

as derived in [4] and reproduced in (2.17).

Having reproduced the result for single-trace theories we can easily show that all non-planar and pinched contributions to the multi-trace effective superpotential vanish. Consider any diagram with ℓ momentum loops and h index loops. By the same arguments as above, we attach some $\mathcal{W}_{(p)}$ to each index loop as in (2.27), and again, the ‘center of mass’ decouples due to the commutator nature of the propagator. Therefore, in the momentum integrals, only $h - 1$ inequivalent $\mathcal{W}_{(p)}$ appear. By doing ℓ momentum integrals, we generate a polynomial of order 2ℓ in the $h - 1$ inequivalent $\mathcal{W}_{(p)}^2$. This polynomial can by Fermi statistics only be non-zero if $\ell \leq h - 1$: $\mathcal{W}_{(p)}^3$ is zero for all p . Therefore, we reach the important conclusion that the total number of index loops must be larger than the number of momentum loops

$$h > \ell \quad (2.34)$$

while the naive selection rule (2.26) says that it could be larger or equal.

Consider pasting and pinching k primitive diagrams together, each with h_i index loops and ℓ_i momentum loops. According to the rules set out in the previous subsection, the total number of index loops and the total number of momentum loops are given by:

$$h = \sum_i h_i \quad ; \quad \ell \geq \sum_i \ell_i \quad (2.35)$$

with equality only when all the primitive diagrams are pasted together without additional momentum loops. Now the total number of independent \mathcal{W} s that appear in full diagram is $\sum_i (h_i - 1)$ since in each primitive diagram the “center of mass” \mathcal{W} will not appear. So the full diagram is non-vanishing only when

$$\ell \leq \sum_i (h_i - 1). \quad (2.36)$$

This inequality is already saturated by the momenta appearing in the primitive diagrams if they are planar. So we can conclude two things. First, only planar primitive diagrams appear in the full diagram. Second, only pasted diagrams are non-vanishing, since pinching introduces additional momentum loops which would violate this inequality.

Summary: The only diagrams that contribute to the effective multi-trace superpotential are pastings of planar primitive diagrams. These are tree-like diagrams which string together double-trace vertices with “propagators” and “external legs” which are themselves primitive diagrams of the single-trace theory. Below we will explicitly evaluate such diagrams and raise the question of whether there is a generating functional for them.

2.4 Summing Pasted Diagrams

In the previous section we generalized steps 7 and 8 of the the single trace case in Sec. 2.1 to the double-trace theory, and found that the surviving diagrams consist of planar connected primitive vacuum graphs pasted together with double-trace vertices. Because of momentum conservation, no momentum can flow through the double-trace vertices in such graphs. Consequently the fermionic integrations and the proof of localization can be carried out separately for each primitive graph, and the entire diagram evaluates to a product of the the primitive components times a suitable power of \tilde{g}_2 , the double-trace coupling.

Let G_i , $i = 1, \dots, k$ be the planar primitive graphs that have been pasted together, each with h_i index loops and $\ell_i = h_i - 1$ momentum loops to make a double-trace diagram G . Then, using the result (2.18) for the single-trace case, the Schwinger parameters in the bosonic and fermionic momentum integrations cancel giving a factor

$$I_{boson} \cdot I_{fermion} = \prod_i (N h_i S_i^{\ell_i}) = N^k S^{\sum_i (h_i - 1)} \prod_i h_i, \quad (2.37)$$

where the last factor arises from the number of ways in which the glueballs S can be inserted into the propagators of each primitive diagram. Defining $C(G) = \prod_i h_i$ as the glueball symmetry factor,

$k(G)$ as the number of primitive components, $h(G) = \sum_i h_i$ as the total number of index loops and $\ell(G) = \sum_i \ell_i = h(G) - k(G)$ as the total number of momentum loops, we get

$$I_{boson} \cdot I_{fermion} = \prod_i (N h_i S_i^{\ell_i}) = N^{h(G)-\ell(G)} S^{\ell(G)} C(G). \quad (2.38)$$

We can assemble this with the Veneziano-Yankielowicz contribution contribution for pure gauge theory [25] to write the complete glueball effective action as

$$W_{eff} = -NS(\log(S/\Lambda^2) - 1) + \sum_G C(G) \mathcal{F}(G) N^{h(G)-\ell(G)} S^{\ell(G)}, \quad (2.39)$$

where $\mathcal{F}(G)$ is the combinatorial factor for generating the graph G from the Feynman diagrams of the double-trace theory. Notice that in our discussion, we have set $g_2 = m = 1$, so Λ^2 in this equation is in fact $m\Lambda^2$ which matches the dimension of S . We can define a free energy related to above diagrams as

$$\mathcal{F}_0 = \sum_G \mathcal{F}(G) S^{h(G)}. \quad (2.40)$$

\mathcal{F}_0 is a generating function for the diagrams that contribute to the effective superpotential, but does not include the combinatorial factors arising from the glueball insertions. In the single-trace case that combinatorial factor was simply $Nh(G)$ and so we could write $W_{eff} = N(\partial\mathcal{F}_0/\partial S)$. Here $C(G) = \prod h_i$ is a product rather than a sum $h(G) = \sum h_i$, and so the effective superpotential cannot be written as a derivative of the free energy.

Notice that if we rescale \tilde{g}_2 to \tilde{g}_2/N , there will be a $N^{-(k(G)-1)}$ factor from $k(G) - 1$ insertions of the double-trace vertex. This factor will change the $N^{h(G)-\ell(G)}$ dependence in (2.39) to just N for every diagram. This implies that the matrix diagrams contributing to the superpotential are exactly those that survive the large M limit of a bosonic $U(M)$ Matrix model with a potential

$$V(\Phi) = g_2 \text{Tr}(\Phi^2) + g_4 \text{Tr}(\Phi^4) + \frac{\tilde{g}_2}{M} \text{Tr}(\Phi^2) \text{Tr}(\Phi^2). \quad (2.41)$$

In Sec. 4 we will compute the large M limit of a such a Matrix model and compute the free energy \mathcal{F}_0 in this way.

Below we will compute this effective action (2.39) to the first few orders. In Sec. 3 we will show that it is reproduced by an analysis based on the Seiberg-Witten solution of $\mathcal{N} = 2$ gauge theories. In the single-trace case Dijkgraaf and Vafa argued that the large- N limit of an associated Matrix model carries out the sum in (2.39), or equivalently, that the matrix model free energy provides a generating function for the perturbative series of matrix diagrams contributing to the exact field theory superpotential. In Sec. 4 we will show that the well known double-trace Matrix models that have large- N limits do sum up the same ‘‘planar pasted diagrams’’ that we described above and give the free energy defined by (2.40). However, unlike the single-trace case, the Matrix model will not reproduce the the combinatorial factors $C(G)$ appearing in (2.39).

2.5 Perturbative Calculation

Thus equipped, let us begin our explicit perturbation calculations. We shall tabulate all combinatoric data of the pasting diagrams up to third order. Here $C(G) = \prod_i h_i$ and $\mathcal{F}(\mathcal{G})$ is obtained by counting the contractions of Φ s. For pure single-trace diagrams the values of $\mathcal{F}(\mathcal{G})$ have been computed in Table 1 in [26], so we can utilize their results.

2.5.1 First Order

To first order in coupling constants, all primitive (diagram (b)) and pasting diagrams (diagram (a)) are presented in Figure 4. Let us illustrate by showing the computations for (a). There is a total of four index loops and hence $h = 4$ for this diagram. Moreover, since it is composed of the pasting of two primitive diagrams each of which has $h = 2$; thus, we have $C(G) = 2 \times 2 = 4$. Finally, $\mathcal{F} = \tilde{g}_2$ because there is only one contraction possible, *viz.*, $\text{Tr}(\overline{\Phi\Phi})\text{Tr}(\overline{\Phi\Phi})$.

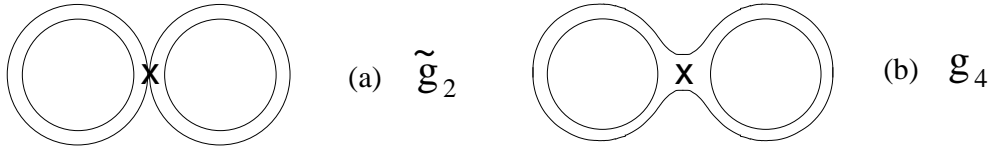


Figure 4: All two-loop primitive and pasting diagrams. The vertices have been marked with a cross.

In summary we have:

diagram	(a)	(b)
h	4	3
$C(G)$	4	3
$\mathcal{F}(G)$	\tilde{g}_2	$2g_4$

(2.42)

2.5.2 Second Order

To second order in the coupling all primitive ((c) and (d)) and pasting diagrams ((a) and (b)) are drawn in Figure 5 and the combinatorics are summarized in table (2.43). Again, let us do an illustrative example. Take diagram (b), there are five index loops, so $h = 5$; more precisely it is composed of pasting a left primitive diagram with $h = 3$ and a right primitive with $h = 2$, so $C(G) = 2 \times 3 = 6$. Now for $\mathcal{F}(G)$, we need contractions of the form $\text{Tr}(\overline{\Phi\Phi} \overline{\Phi\Phi})\text{Tr}(\overline{\Phi\Phi})\text{Tr}(\overline{\Phi\Phi})$; there are $4 \times 2 \times 2 = 16$ ways of doing so. Furthermore, for this even overall power in the coupling, we have a minus sign when expanding out the exponent. Therefore $\mathcal{F}(G) = -16\tilde{g}_2g_4$ for this diagram.

In summary, we have:

diagram	(a)	(b)	(c)	(d)
h	6	5	4	4
$C(G)$	8	6	4	4
$\mathcal{F}(G)$	$-4\tilde{g}_2^2$	$-16\tilde{g}_2g_4$	$-2g_4^2$	$-16g_4^2$

(2.43)

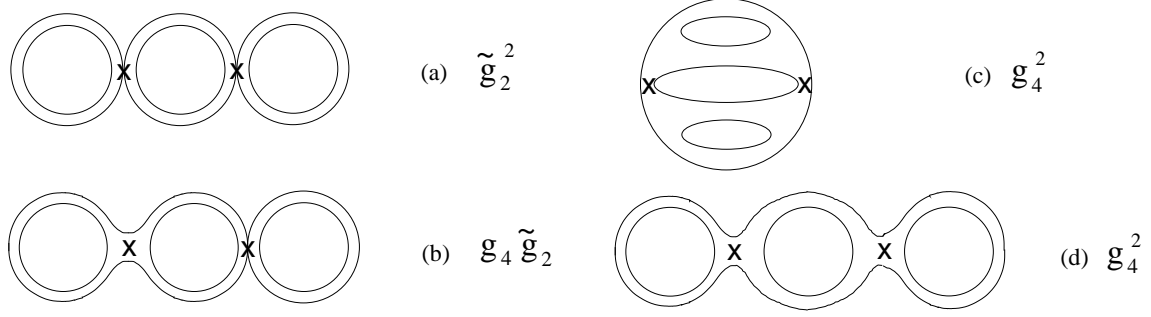


Figure 5: All three-loop primitive and pasting diagrams. The vertices have been marked with a cross.

2.5.3 Third Order

Finally, the third order diagrams are drawn in Figure 6. The combinatorics are tabulated in (2.44). Here the demonstrative example is diagram (b), which is composed of pasting four diagrams, each with $h = 2$, thus $h(G) = 4 \times 2 = 8$ and $C(G) = 2^4 = 16$. For $\mathcal{F}(G)$, first we have a factor $\frac{1}{3!}$ from the exponential. Next we have contractions of the form $\overline{\text{Tr}(\Phi\Phi)^3 \text{Tr}(\Phi\Phi) \text{Tr}(\Phi\Phi) \text{Tr}(\Phi\Phi)}$; there are $2^3 \times 4 \times 2$ ways of doing this. Thus altogether we have $\mathcal{F}(G) = \frac{32}{3} \tilde{g}_2^3$ for this diagram.

In summary:

diagram	(a)	(b)	(c)	(d)	(e)	(f)	(g)	
h	8	8	7	7	7	6	6	
$C(G)$	16	16	12	12	12	8	8	
$\mathcal{F}(G)$	$16\tilde{g}_2^3$	$\frac{32}{3}\tilde{g}_2^3$	$64\tilde{g}_2^2 g_4$	$32\tilde{g}_2^2 g_4$	$64\tilde{g}_2^2 g_4$	$128\tilde{g}_2 g_4^2$	$128\tilde{g}_2 g_4^2$	(2.44)
diagram	(h)	(i)	(j)	(k)	(l)	(m)		
h	6	6	5	5	5	5		
$C(G)$	8	9	5	5	5	5		
$\mathcal{F}(G)$	$32\tilde{g}_2 g_4^2$	$64\tilde{g}_2 g_4^2$	$128g_4^3$	$\frac{32}{3}g_4^3$	$64g_4^3$	$\frac{256}{3}g_4^3$		

2.5.4 Obtaining the Effective Action

Now to the highlight of our calculation. From tables (2.42), (2.43), and (2.44) we can readily compute the effective glueball superpotential and free energy. We do so by summing the factors, with the appropriate powers for S , in accordance with (2.39,2.40).

We obtain, up to four-loop order,

$$\begin{aligned}
\mathcal{F}_0 &= \sum_{G=\text{all diagrams}} \mathcal{F}(G) S^{h(G)} \\
&= (2g_4 + \tilde{g}_2 S) S^3 - 2(9g_4^2 + 8g_4 \tilde{g}_2 S + 2\tilde{g}_2^2 S^2) S^4 \\
&\quad + \frac{16}{3} (54g_4^3 + 66g_4^2 \tilde{g}_2 S + 30g_4 \tilde{g}_2^2 S^2 + 5\tilde{g}_2^3 S^3) S^5 + \dots,
\end{aligned} \tag{2.45}$$

and subsequently,

$$W_{eff} = -NS(\log(S/\Lambda^2) - 1) + \sum_{G=\text{all diagrams}} C(G) \mathcal{F}(G) N^{h(G)-l(G)} S^{l(G)}$$

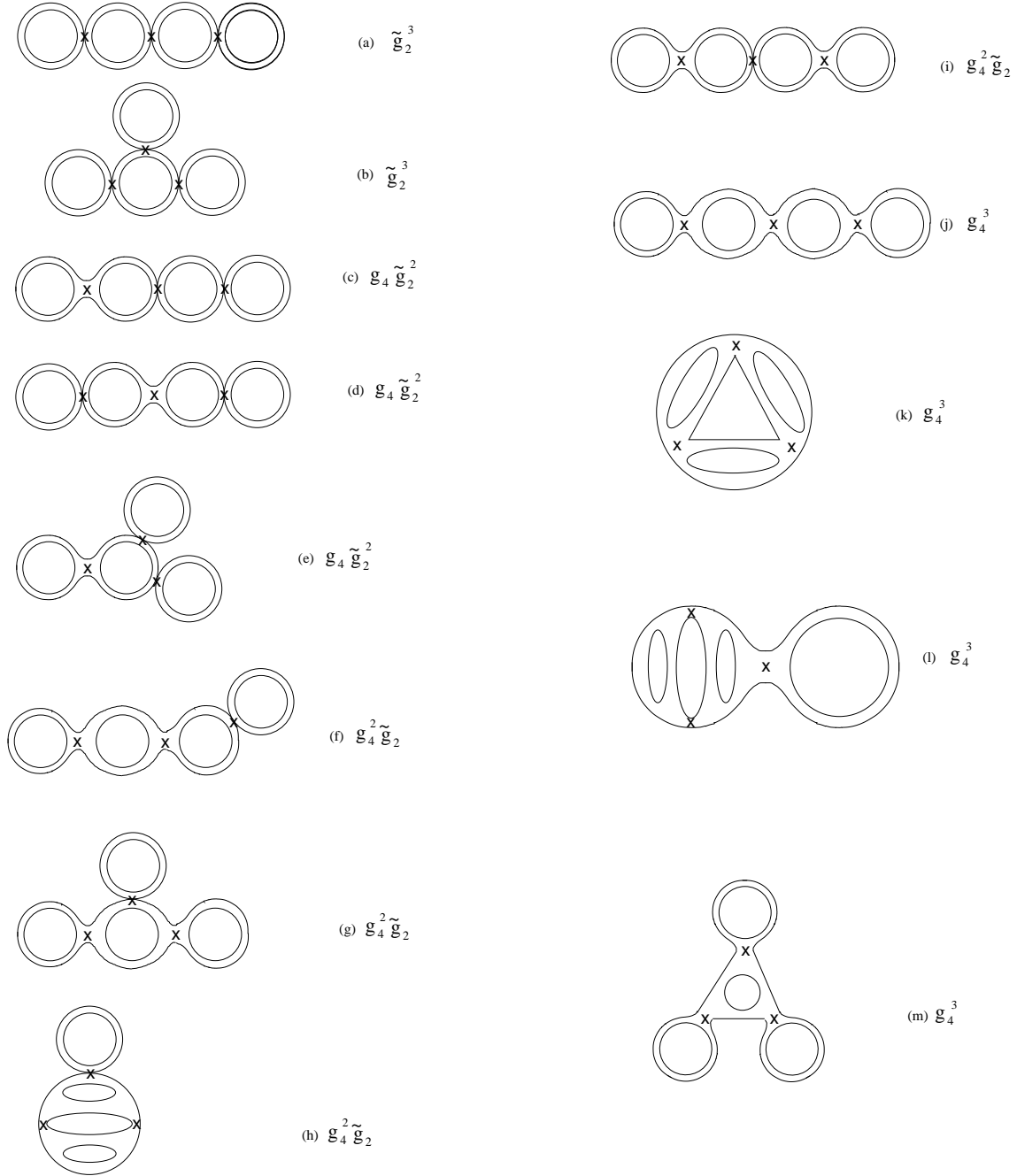


Figure 6: All four-loop primitive and pasting diagrams. The vertices have been marked with a cross.

$$\begin{aligned}
&= -NS(\log(S/\Lambda^2) - 1) + (6g_4 + 4\tilde{g}_2 N)NS^2 - (72g_4^2 + 96g_4\tilde{g}_2 N + 32\tilde{g}_2^2 N^2)NS^3 \\
&\quad + \frac{20}{3}(6g_4 + 4\tilde{g}_2 N)^3 NS^4 + \dots
\end{aligned} \tag{2.46}$$

We will later see how this result may be reproduced from independent considerations, *i.e.*, the effective action from the factorization of Seiberg-Witten curve and free energy from the corresponding matrix model.

2.6 Multiple Traces, Pasted Diagrams and Nonlocality

Above we found that the only diagrams that contribute to the effective superpotential have zero momentum flowing through the double-trace vertex. Now observe that the double-trace term in the tree-level action can be written in momentum space as:

$$\begin{aligned} V &= \int d^4x \operatorname{Tr}(\Phi^2(x))\operatorname{Tr}(\Phi^2(x)) \\ &= \int d^4p_1 d^4p_2 d^4p_3 d^4p_4 \operatorname{Tr}(\Phi(p_1)\Phi(p_2))\operatorname{Tr}(\Phi(p_3)\Phi(p_4)) \delta(p_1 + p_2 + p_3 + p_4). \end{aligned} \quad (2.47)$$

Since no momentum flows through the double-trace vertices contributing to the superpotential, the delta function momentum constraint factorizes in our pasted diagrams as

$$\delta(p_1 + p_2 + p_3 + p_4) \sim \delta(p_1 + p_2)\delta(p_3 + p_4). \quad (2.48)$$

Therefore for the purposes of computing the superpotential we might as well replace the double-trace term in the action by

$$\begin{aligned} \tilde{V} &= \int d^4p_1 d^4p_2 d^4p_3 d^4p_4 \operatorname{Tr}(\Phi(p_1)\Phi(p_2))\operatorname{Tr}(\Phi(p_3)\Phi(p_4)) \delta(p_1 + p_2) \delta(p_3 + p_4) \\ &= \int d^4x d^4y \operatorname{Tr}(\Phi^2(x))\operatorname{Tr}(\Phi^2(y)). \end{aligned} \quad (2.49)$$

The Feynman diagrams of this *nonlocal* theory include the ones that compute the superpotential in the double-trace, local theory.

This fact suggests that correlation functions of chiral operators are position independent, as described in [5]. Along with cluster decomposition, this position independence leads to the statement that correlators of operators in the chiral ring of an $\mathcal{N} = 1$ theory factorize, which we use in the next section to write $\langle \operatorname{Tr}(\Phi^2)^2 \rangle = \langle \operatorname{Tr}(\Phi^2) \rangle^2$. However it is subtle to establish the precise equivalence between factorization of chiral operators and the vanishing that we demonstrated of all except the pasted diagrams, which leads in turn to the nonlocal action in (2.49). We leave this potential connection for exploration in future work.

3. The Field Theory Analysis

In this section, we will show that in the confining vacuum the effective superpotential of the field theory discussed in the previous section is

$$W_{eff} = N\Lambda^2 + (6Ng_4 + 4N^2\tilde{g}_2)\Lambda^4. \quad (3.1)$$

After integrating in the glueball superfield and expanding the superpotential in a power series in S , (3.1) can be written

$$W_{eff} = -NS(\log(S/\Lambda^2) - 1) + (6g_4 + 4\tilde{g}_2N)NS^2 - 2(6g_4 + 4\tilde{g}_2N)^2NS^3 + \frac{20}{3}(6g_4 + 4\tilde{g}_2N)^3NS^4 + \dots \quad (3.2)$$

We shall compare this expression for the low-energy gauge dynamics to the perturbative field theory computations in Sec. 2. The two results, of course, are in concert.

We begin by considering an $\mathcal{N} = 1$ $U(N)$ gauge theory with a single adjoint superfield Φ deformed from $\mathcal{N} = 2$ by the tree-level superpotential ($n < N$)

$$W_{tree} = \sum_{r=1}^{n+1} g_r u_r + 4\tilde{g}_2 u_2^2, \quad (3.3)$$

where

$$u_k := \frac{1}{k} \text{Tr}(\Phi^k). \quad (3.4)$$

The tree-level superpotential in (3.3) is more general than the one used in (2.23). Here, we allow single-trace terms at arbitrary powers of Φ . We shall specialize to the previous example at the end of our discussion.

3.1 The Classical Vacua

To find the classical vacua, we have to solve the D-term and F-term conditions. The D-term is proportional to $\text{Tr}[\Phi, \bar{\Phi}]^2$ which is zero if Φ is diagonal. Let the diagonal entries be x_i , $i = 1, \dots, N$. We still need to solve the F-term condition. In terms of the x_i , the tree-level superpotential is

$$W = \sum_{r=1}^{n+1} \frac{g_r}{r} \sum_{i=1}^N x_i^r + \tilde{g}_2 \left(\sum_{i=1}^N x_i^2 \right)^2. \quad (3.5)$$

From this, the F-flatness condition reads:

$$0 = \frac{\partial W}{\partial x_k} = \sum_{r=1}^{n+1} g_r x_k^{r-1} + 4\tilde{g}_2 x_k \left(\sum_{i=1}^N x_i^2 \right), \quad k = 1, \dots, N. \quad (3.6)$$

This is certainly different from the case without the double-trace term, where the F-term equations for different x_k s decouple. Here, the eigenvalues interact with each other even at the classical level.

To solve the (3.6), which may be recast as

$$\frac{1}{x_k} \sum_{r=1}^{n+1} g_r x_k^{r-1} = -4\tilde{g}_2 \left(\sum_{i=1}^N x_i^2 \right), \quad (3.7)$$

we take the RHS of (3.7)

$$C := 4\tilde{g}_2 \left(\sum_{i=1}^N x_i^2 \right), \quad (3.8)$$

as an unknown constant for all N F-terms. This gives

$$\sum_{r=1}^{n+1} g_r x_k^{r-1} + C x_k = 0 \quad \forall k. \quad (3.9)$$

Now the F-terms are decoupled. We can solve this system just as we solve for the vacua of a field theory with only single-trace interactions [28] simply by taking $g_2 \mapsto g_2 + C$.

As the F-terms are order n polynomials in x , we should generically expect n solutions for each eigenvalue x_k . The eigenvalues are the roots of the polynomial

$$0 = \sum_{r=1}^{n+1} g_r x_k^{r-1} \equiv g_{n+1} \prod_{i=1}^n (x - a_i). \quad (3.10)$$

If N_i of the eigenvalues are located at a_i , where $\sum_i N_i = N$, the unbroken gauge symmetry is

$$U(N) \rightarrow \prod_{i=1}^n U(N_i). \quad (3.11)$$

As a_i s are a function of C , we need to impose the *additional* consistency condition that

$$4\tilde{g}_2 \sum_{j=1}^n N_j^2 a_j^2 = C. \quad (3.12)$$

To simplify the discussion, we henceforth focus on the special case where all of the x_i s have the same value. The $SU(N)$ part of the gauge group is unbroken, and will confine in the infrared.

3.2 The Exact Superpotential in the Confining Vacuum

We now proceed to find the exact superpotential in this confining vacuum [27]. Let us recall the general philosophy of the method (see *e.g.*, [29], whose notations we adopt, for a recent discussion). A generic point in the moduli space of the $U(N)$ $\mathcal{N} = 2$ theory will be lifted by the addition of the the general superpotential (3.3). The points which are not lifted are precisely where at least $N - n$ mutually local monopoles become massless. This can be seen from the following argument. The gauge group in the $\mathcal{N} = 1$ theory is broken down to $\prod_{i=1}^n U(N_i)$, and the $SU(N_i)$ factors each confine. We expect condensation of $N_i - 1$ magnetic monopoles in each of these $SU(N_i)$ factors and a total of $N - n$ condensed magnetic monopoles. These monopoles condense at the points on the $\mathcal{N} = 2$ moduli space where $N - n$ mutually local monopoles become massless. These are precisely the points which are not lifted by addition of the superpotential. These considerations are equivalent to the requirement that the corresponding Seiberg-Witten curve has the factorization

$$P_N(x, u)^2 - 4\Lambda^{2N} = H_{N-n}(x)^2 F_{2n}(x), \quad (3.13)$$

where $P_N(x, u)$ is an order N polynomial in x with coefficients determined by the (vevs of) the u_k , Λ is an ultraviolet cut-off, and H and F are, respectively, order $N - n$ and $2n$ polynomials in x .

The $N - n$ double roots place $N - n$ conditions on the original variables u_k . We can parametrize all the $\langle u_k \rangle$ by n independent variables α_j . In other words, the α_j s then correspond to massless fields in the low-energy effective theory. If we know the exact effective action for these fields, to find the vacua, we simply minimize S_{eff} . Furthermore, substituting $\langle u_k \rangle$ back into the effective action gives the action for the vacua.

Holomorphy and regularity of the superpotential as the couplings go to zero requires that there are no perturbative corrections to the tree-level superpotential. In addition, we assume that all

non-perturbative effects are captured in the Seiberg-Witten curve analysis discussed above. Then, we need to minimize

$$W_{exact} = \sum_{r=1}^{n+1} g_r \langle u_r \rangle + 4\tilde{g}_2 \langle u_2^2 \rangle. \quad (3.14)$$

In general the factorization problem is hard to solve [30], but for the confining vacuum where all $N - 1$ monopoles have condensed, there is a general solution given by Chebyshev polynomials.² In our case, we have the solution

$$u_p = \frac{N}{p} \sum_{q=0}^{[p/2]} C_p^{2q} C_{2q}^q \Lambda^{2q} z^{p-2q}, \quad (3.15)$$

$$z = \frac{u_1}{N}, \quad C_n^p := \binom{n}{p} = \frac{n!}{p!(n-p)!}. \quad (3.16)$$

Notice that in (3.15), there is one free parameter z which is the field left upon condensation. Now we put it into the superpotential

$$W = \sum_{r=1}^{n+1} g_r u_r(z, \Lambda) + 4\tilde{g}_2 u_2(z, \Lambda)^2, \quad (3.17)$$

solve and back-substitute z from $\partial W / \partial z = 0$ to obtain the effective superpotential W_{eff} . Notice that in the above result, we have used

$$\langle u_2^2 \rangle = \langle u_2 \rangle^2. \quad (3.18)$$

This is true because u_2 is a chiral field, and cluster decomposition in the field theory lets us factor the correlation functions of operators in the chiral ring [5].

Although the above procedure finds W_{eff} , it is not the best form to compare with our previous results because there is no gluino condensate S . To make the comparison, we need to “integrate in” [31] the glueball superfield as in [29].

The integrating in procedure is as follows (here we use the single-trace superpotential as an illustrative example of the technique).

- We set $\Delta := \Lambda^2$, and use the equation

$$NS = \Delta \frac{\partial W}{\partial \Delta} = N \sum_{r=2}^{n+1} g_r \sum_{q=1}^{[p/2]} \frac{q}{p} C_p^{2q} C_{2q}^q z^{p-2q} \Delta^q \quad (3.19)$$

to solve for Δ in terms of S .

- Next, we find z by solving

$$0 = \frac{\partial W}{\partial z} = \sum_{r=1}^{n+1} g_r \sum_{q=0}^{[p/2]} \frac{p-2q}{p} C_p^{2q} C_{2q}^q z^{p-2q-1} \Delta^q. \quad (3.20)$$

²This was worked out first by Douglas and Shenker [32], but here we use the results and nomenclature of Ferrari [29].

- Now the effective action for the glueball superfield S can be written as

$$W_S(S, g, \Lambda) = -S \log \left(\frac{\Delta}{\Lambda^2} \right)^N + W_{tree}(S, g, \Lambda), \quad (3.21)$$

which will reproduce the result

$$\frac{\partial}{\partial S} W_S(S, \Lambda^2, g) = -\ln(\Delta/\Lambda^2)^N. \quad (3.22)$$

3.3 An Explicit Example

Let us work out the double-trace example that we are interested in solving. The superpotential is

$$W = g_2 u_2 + 4g_4 u_4 + 4\tilde{g}_2 u_2^2, \quad (3.23)$$

(later, we can set $g_2 = m = 1$). Using

$$u_2 = \frac{N}{2}[z^2 + 2\Lambda^2], \quad (3.24)$$

$$u_4 = \frac{N}{4}[z^4 + 12\Lambda^2 z^2 + 6\Lambda^4], \quad (3.25)$$

from (3.15), we obtain

$$\begin{aligned} W = N z^2 \left[\frac{g_2}{2} + g_4 z^2 + 12g_4 \Lambda^2 + 4N\tilde{g}_2 \Lambda^2 + N\tilde{g}_2 z^2 \right] \\ + N \Lambda^2 [g_2 + 6g_4 \Lambda^2 + 4N\tilde{g}_2 \Lambda^2]. \end{aligned} \quad (3.26)$$

From this we have following equations by setting $\Lambda^2 = \Delta$:

$$S = \Delta [g_2 + (12g_4 + 4N\tilde{g}_2)z^2 + (12g_4 + 8N\tilde{g}_2)\Delta], \quad (3.27)$$

$$0 = \frac{\partial W}{\partial z} = z [g_2 + z^2(4g_4 + 4N\tilde{g}_2) + 2\Delta(12g_4 + 4N\tilde{g}_2)]. \quad (3.28)$$

We solve $z = 0$:

$$\Delta = \frac{-g_2 + \sqrt{g_2^2 + 4S(12g_4 + 8N\tilde{g}_2)}}{2(12g_4 + 8N\tilde{g}_2)}. \quad (3.29)$$

The effective action with S integrated in is³

$$W_{eff} = S \log \left(\frac{\Lambda^2}{\Delta} \right)^N + N \Delta [g_2 + \Delta(6g_4 + 4N\tilde{g}_2)], \quad (3.30)$$

which will be the one used in comparison to our previous results. After minimizing this action, we find

$$W_{z=0} = N \Lambda^2 [g_2 + 6g_4 \Lambda^2 + 4N\tilde{g}_2 \Lambda^2], \quad (3.31)$$

³Notice that in both formula (3.29) and (3.30), g_4 and \tilde{g}_2 combine together as $g_4 + \frac{2N}{3}\tilde{g}_2$. So if we shift g_4 to $g_4 + \frac{2N}{3}\tilde{g}_2$, the single-trace result will reproduce the double-trace result, and the effective action for the double-trace can be naively calculated from the DV prescription by partial differentiation of the glueball field S .

which is the promised result of (3.1). Setting $g_2 = 1$, expanding (3.29) in powers of S , and substituting into (3.30), we get the second formula (3.2) from the beginning of this section:

$$W_{eff} = -NS(\log(S/\Lambda^2) - 1) + (6g_4 + 4\tilde{g}_2 N)NS^2 - 2(6g_4 + 4\tilde{g}_2 N)^2 NS^3 + \frac{20}{3}(6g_4 + 4\tilde{g}_2 N)^3 NS^4 + \dots \quad (3.32)$$

Crucial in matching the result of this calculation with the perturbative analysis in the previous section is the assumption of factorization $\langle u_2^2 \rangle = \langle u_2 \rangle^2$. This is equivalent to the vanishing the pinching diagrams in the perturbative analysis.

4. The Matrix Model

In Sec. 2 we demonstrated that the explicit field theory computation of the effective superpotential localizes to a certain sum of matrix diagrams. All of these diagrams are constructed by pasting planar single-trace diagrams together with double-trace vertices in such a way that no additional momentum loops are created. By examining the scaling of these diagrams with N in (2.39) we also observed that these are precisely the diagrams that would survive the large- M limit of a $U(M)$ bosonic Matrix model with a potential

$$V(\Phi) = g_2 \text{Tr}(\Phi^2) + g_4 \text{Tr}(\Phi^4) + \frac{\tilde{g}_2}{M} \text{Tr}(\Phi^2) \text{Tr}(\Phi^2). \quad (4.1)$$

The extra factor of $1/M$ multiplying \tilde{g}_2 , in comparison with the field theory tree-level superpotential (1.1) is necessary for a well-defined 't Hooft large- M limit. This is because each trace, being a sum of eigenvalues, will give a term proportional to M . So to prevent the double-trace term from completely dominating the large- M limit we must divide by an extra factor of M . Fortunately, this a well known model and was solved more than a decade ago [22, 33]. Below we will review this solution, compare its results to our field theory calculations, and then generalize to other multi-trace deformations.

4.1 The Mean-Field Method

The basic observation, following [22], that allows us to solve the double-trace matrix model (4.1), is that in the large- M limit the effects on a given matrix eigenvalue of all the other eigenvalues can be treated in a mean field approximation. Accordingly we compute the matrix model free energy \mathcal{F} as

$$\begin{aligned} \exp(-M^2 \mathcal{F}) &= \int d^{M^2}(\Phi) \exp\left\{-M\left(\frac{1}{2}\text{Tr}(\Phi^2) + g_4 \text{Tr}(\Phi^4) + \tilde{g}_2 \frac{(\text{Tr}(\Phi^2))^2}{M}\right)\right\}. \quad (4.2) \\ &= \int \prod_i d\lambda_i \exp\left\{M\left(-\frac{1}{2} \sum_i \lambda_i^2 - \frac{g_4}{M} \sum_i \lambda_i^4 - \frac{\tilde{g}_2}{M^2} \left(\sum_i \lambda_i^2\right)^2 + \sum_{i \neq j} \log |\lambda_i - \lambda_j|\right)\right\} \end{aligned}$$

Here λ are the M eigenvalues of Φ and \mathcal{F} is the free energy, which can be evaluated by saddle point approximation at the planar limit. The log term comes from the standard Vandermonde determinant. This matrix model is Hermitian with rank M in the notation of [35] (of course

as mentioned earlier, we should really consider $GL(M, \mathbb{C})$ matrices though the techniques hold equally). We have introduced an extra factor of M in the exponent on the right hand side of (4.2) by rescaling the fields and couplings in (4.1) in accordance with the conventions of [22].

The density of eigenvalues

$$\rho(\lambda) := \frac{1}{M} \sum_{i=1}^M \delta(\lambda - \lambda_i) \quad (4.3)$$

becomes continuous in an interval $(-2a, 2a)$ when M goes to infinity in the planar limit for some $a \in \mathbb{R}^+$. Here the interval is symmetric around zero since our model is an even function. The normalization condition for eigenvalue density is

$$\int_{-2a}^{2a} d\lambda \rho(\lambda) = 1. \quad (4.4)$$

We can rewrite (4.2) in terms of the eigenvalue density in the continuum limit as

$$\begin{aligned} \exp(-M^2 \mathcal{F}) &= \int \prod_{i=1}^M d\lambda_i \exp\left\{-M^2 \left(\int_{-2a}^{2a} d\lambda \rho(\lambda) \left(\frac{1}{2} \lambda^2 + g_4 \lambda^4 \right) \right. \right. \\ &\quad \left. \left. + \tilde{g}_2 \left(\int_{-2a}^{2a} d\lambda \rho(\lambda) \lambda^2 \right)^2 - \int_{-2a}^{2a} \int_{-2a}^{2a} d\lambda d\mu \rho(\lambda) \rho(\mu) \ln |\lambda - \mu| \right) \right\}. \end{aligned} \quad (4.5)$$

Then the saddle point equation is

$$\frac{1}{2} \lambda + 2g_4 \lambda^3 + 2\tilde{g}_2 c \lambda = P \int_{-2a}^{2a} d\mu \frac{\rho(\mu)}{\lambda - \mu}, \quad (4.6)$$

where c is the second moment

$$c := \int_{-2a}^{2a} d\lambda \rho(\lambda) \lambda^2 \quad (4.7)$$

and P means principal value integration.

The effect of the double-trace is to modify the coefficient of λ in the saddle point equation. We can determine the number c self-consistently by (4.7). The solution of $\rho(\lambda)$ to (4.6) can be obtained by standard matrix model techniques by introducing a resolvent. The answer is

$$\rho(\lambda) = \frac{1}{\pi} \left(\frac{1}{2} + 2\tilde{g}_2 c + 4g_4 a^2 + 2g_4 \lambda^2 \right) \sqrt{4a^2 - \lambda}. \quad (4.8)$$

Plugging the solution into (4.4) and (4.7) we obtain two equations that determine the parameters a and c :

$$a^2(1 + 4\tilde{g}_2 c) = 1 - 12g_4 a^4, \quad (4.9)$$

$$16g_4 \tilde{g}_2 a^8 + (12g_4 + 4\tilde{g}_2) a^4 + a^2 - 1 = 0. \quad (4.10)$$

Substituting these expressions into (4.5) gives us the free energy in the planar limit $M \rightarrow \infty$ as:

$$\mathcal{F} = \int_{-2a}^{2a} d\lambda \rho(\lambda) \left(\frac{1}{2} \lambda^2 + g_4 \lambda^4 \right) + \tilde{g}_2 c^2 - \int \int_{-2a}^{2a} d\lambda d\mu \rho(\lambda) \rho(\mu) \ln |\lambda - \mu|. \quad (4.11)$$

One obtains

$$\mathcal{F}(g_4, \tilde{g}_2) - \mathcal{F}(0, 0) = \frac{1}{4}(a^2 - 1) + (6g_4a^4 + a^2 - 2)g_4a^4 - \frac{1}{2}\log(a^2). \quad (4.12)$$

Equation (4.12) together with (4.10) give the planar free energy. We can also expand the free energy in powers of the couplings, by using (4.10) to solve for a^2 perturbatively

$$\begin{aligned} a^2 = & 1 - (12g_4 + 4\tilde{g}_2) + (288g_4^2 + 176g_4\tilde{g}_2 + 32\tilde{g}_2^2) \\ & - (8640g_4^3 + 7488g_4^2\tilde{g}_2 + 2496g_4\tilde{g}_2^2 + 320\tilde{g}_2^3) + \dots \end{aligned} \quad (4.13)$$

Plugging this back into (4.12) we find the free energy as a perturbative series

$$\mathcal{F}_0 = \mathcal{F}(g_4, \tilde{g}_2) - \mathcal{F}(0, 0) = 2g_4 + \tilde{g}_2 - 2(9g_4^2 + 8g_4\tilde{g}_2 + 2\tilde{g}_2^2) + \frac{16}{3}(54g_4^3 + 66g_4^2\tilde{g}_2 + 30g_4\tilde{g}_2^2 + 5\tilde{g}_2^3) + \dots \quad (4.14)$$

Comparing with (2.45) we see that \mathcal{F} reproduces the explicit computation of the generating function of “planar pasted” field theory diagrams in Sec. 2.5. In matching the two we have to restore the proper powers of the glueball S into (4.14). First recall that to keep the relevant diagrams in the matrix model, we have inserted $\frac{1}{M}$ to the double-trace term in (4.1). Therefore to compare with (2.45), we need to rescale \tilde{g}_2 in (4.14) to $\tilde{g}_2 M \equiv \tilde{g}_2 S$ where we have effectively identified the glueball S in the field theory with M in the matrix model. In addition, we should re-insert powers of M into (4.14) by loop counting. The first two terms in (4.14) have three index loops so we need to multiply them by $M^3 \equiv S^3$. The third term has four index loops and fourth term, five and hence we respectively need factors of S^4 and S^5 . With these factors correctly placed into (4.14), we recover (2.45) completely.

This verifies our claim that the diagrams surviving the large- M limit of the matrix model (4.1) are precisely the graphs that contribute to effective action of the field theory with the tree-level superpotential (1.1). Nevertheless, as we have already discussed in Sec. 2.4 we cannot compute the effective superpotential of the field theory $W_{eff}(S)$ by taking a derivative $\partial\mathcal{F}_0/\partial S$, because the combinatorial factors will not agree. In this way the double-trace theories differ in a significant way from the single-trace models discussed by Dijkgraaf and Vafa [3]. We can pose the challenge of finding the field theories whose effective superpotential is computed by the Matrix model (4.12).

4.2 Generalized Multi-Trace Deformations

In fact the mean field techniques of the previous subsection can be generalized to solve the general multi-trace model. Below we illustrate this by solving the general quartic Matrix model; as discussed above, it is an interesting challenge to find a field theory whose effective superpotential these models compute.

Specifically, let us consider the Lagrangian

$$\mathcal{L} = g_2 \text{Tr}(\Phi)^2 + \mu(\text{Tr}(\Phi))^2 + \nu_1(\text{Tr}\Phi)^2(\text{Tr}(\Phi^2)) + \nu_2(\text{Tr}\Phi)^4 + 2\nu_3(\text{Tr}\Phi)(\text{Tr}(\Phi^3)), \quad (4.15)$$

which exhausts all quartic interactions.

The one-matrix model partition function

$$Z_M = \int [D\lambda] \exp \left\{ -M^2 \left(\mathcal{L} - \int_0^1 dx \int_0^1 dy \log |\lambda(x) - \lambda(y)| \right) \right\}, \quad (4.16)$$

gives the saddle point equation

$$4g_4\lambda^3 + 6\nu_3c_1\lambda^2 + 2(g_2 + 2\tilde{g}_2c_2 + \nu_1c_1^2)\lambda + 2(\mu c_1 + \nu_1c_1c_2 + 2\nu_2c_1^3 + \nu_3c_3) = 2P \int_{-2a}^{2b} d\tau \frac{u(\tau)}{\lambda - \tau}, \quad (4.17)$$

where the moments c_k are defined as

$$\begin{aligned} c_k &= \int_{-2a}^{2b} d\tau u(\tau) \tau^k, \\ c_0 &= \int_{-2a}^{2b} d\tau u(\tau) = 1. \end{aligned} \quad (4.18)$$

Note that we have introduced the separate upper and lower cut parameters a and b as opposed to the standard symmetric treatment because $u(\lambda)$ is not of explicit parity (such asymmetric examples have also been considered in [26]). When $a = b$ one can recast (4.17) into a Fredholm integral equation of the first kind and Cauchy type, which affords a general solution as follows [36]

$$P \frac{1}{\pi} \int_{-a}^a \frac{u(t) dt}{t - x} = -v(x) \Rightarrow u(x) = \frac{1}{\pi} \int_{-a}^a \left(\sqrt{\frac{a^2 - t^2}{a^2 - x^2}} \right) \frac{v(t) dt}{t - x} + \frac{C}{\sqrt{a^2 - x^2}} \quad (4.19)$$

for some constant C . When $a \neq b$ we can use the ansatz:

$$u(\lambda) = \frac{1}{\pi} (A\lambda^2 + B\lambda + C) \sqrt{(2a + \lambda)(2b - \lambda)} \quad (4.20)$$

with the constants matching the coefficients in the LHS of (4.17) as

$$2A = 2g_4, \quad (4.21)$$

$$2aA - 2Ab + 2B = 3\nu_3c_1,$$

$$-a^2A - 2aAb - Ab^2 + 2aB - 2bB + 2C = g_2 + 2\tilde{g}_2c_2 + \nu_1c_1^2,$$

$$a^3A + a^2Ab - aAb^2 - Ab^3 - a^2B - 2abB - b^2B + 2aC - 2bC = \mu c_1 + \nu_1c_1c_2 + 2\nu_2c_1^3 + \nu_3c_3.$$

We see a well-behaved $u(\lambda)$ which is zero at the end-points and vanishes outside the support $(-2a, 2b)$.

We now need to check the consistency of our mean-field method. This simply means the following. Considering the definition of c_i in (4.18), the definitions (4.21) actually constitute a system of equations for A, B, C, a, b because each c_i on the RHS, through (4.18), depend on A, B, C, a, b . To (4.21) we must append one more normalization condition, that $c_0 = \int_{-2a}^{2b} u(\lambda) d\lambda = 1$. Therefore we have five equations in five variables which will fix our parameters in terms of the seven couplings. Our mean-field method is therefore self-consistent. It would be interesting to find a role for such exactly solvable models in the physics of four-dimensional field theories.

5. Linearizing Traces: How To Identify the Glueball?

In previous sections we showed that the field theory computation of the effective superpotential of a double-trace theory as a function of the glueball S localized to summing Matrix diagrams. In the end, the only the “pasted” diagrams that contributed, namely certain tree-like graphs obtained by pasting together planar single-trace graphs with double-trace vertices in such a way that no momentum flows through the latter. After verifying the result via the $\mathcal{N} = 2$ Seiberg-Witten solution, we demonstrated that the sum of these diagrams given as a series in (2.39) is not computed by the large M limit of a $U(M)$ Matrix as one would have naturally hoped. Nevertheless, we may wonder if there is some Matrix model that sums the series of pasted diagrams. In this section we take up the challenge of finding such a Matrix model.

Since the authors [4] and [5] have proven that the superpotential of a single-trace gauge theory can be computed from an associated Matrix model, we seek to construct our double-trace theory from another single-trace model. Recall that we are considering the tree-level superpotential

$$W_{tree} = \frac{1}{2}g_2\text{Tr}(\Phi^2) + g_4\text{Tr}(\Phi^4) + \tilde{g}_2(\text{Tr}(\Phi^2))^2. \quad (5.1)$$

Now consider another theory with an additional gauge singlet field A

$$W_{tree} = \frac{1}{2}(g_2 + 4\tilde{g}_2A)\text{Tr}(\Phi^2) + g_4\text{Tr}(\Phi^4) - \tilde{g}_2A^2. \quad (5.2)$$

It is easy to see that integrating out A in (5.2), which amounts to solving $\frac{\partial W_{tree}}{\partial A} = 0$ and back-substituting, produces the double-trace theory (5.1).

The advantage of (5.2) is that it consists purely of single-trace operators. The first two terms will generate an effective potential $W_{\text{single}}(A, S)$, as a function of A and the glueball superfield S (the subscript “single” refers to the fact that this is the superpotential for the model without the double-trace term and with an A dependent mass term). Then

$$W_{\text{eff}}(A, S) = W_{\text{single}}(A, S) - \tilde{g}_2A^2. \quad (5.3)$$

The exact superpotential for the glueball superfield S for the double-trace theory then follows by integrating A out, *i.e.* solving $\frac{\partial W_{\text{single}}}{\partial A} - 2\tilde{g}_2A = 0$ for A and substituting in (5.3). Since single-trace theories are directly related to Matrix model we might hope to use this construction with an added auxiliary field A to find an auxiliary Matrix model that sums the pasted diagrams of the double-trace theory.

5.1 Field Theory Computation of $W_{\text{single}}(\mathbf{A}, \mathbf{S})$ and Pasted Matrix Diagrams

In this section⁴ we will discuss how the superpotential for the double-trace theory can be computed in field theory from the linearized model (5.2). First, observe that the superpotential for an adjoint theory with an additional gauge singlet (5.2) localizes to summing matrix integrals, since the arguments of [4] that are reviewed in Sec. 2 go through essentially unchanged. To compute the

⁴We thank Cumrun Vafa and Ken Intriligator for communications concerning the material in this section.

effective potential as a function of both A and the glueball S , we need to sum superspace Feynman diagrams with insertions of both A and \mathcal{W}_α , with both of these treated as background fields. Since we are only interested in contributions to the superpotential, we can restrict ourselves to constant background A . Then it is easy to verify that the entire analysis in Sec. 2 goes through for the theory (5.2), with the double-trace coupling \tilde{g}_2 set to zero and a shift in the mass of the field Φ , *viz* $g_2 \rightarrow g_2 + 4\tilde{g}_2$. In particular, the computation of the effective superpotential $W_{\text{single}}(A, S)$ localizes to summing matrix diagrams and there is some free energy $\mathcal{F}_{\text{single}}$ in terms of which $W_{\text{single}} = N\partial\mathcal{F}_{\text{single}}(S, A)/\partial S$.

Let us verify that this procedure will yield the correct double-trace result when we integrate A out. Making the $g_2 \rightarrow g_2 + 4\tilde{g}_2$ with $\tilde{g}_2 = 0$ in the known single-trace result (3.30) and (3.29), we find the effective superpotential

$$W_{\text{single}}(A, S) = NS \log\left(\frac{\Lambda^2}{\Delta}\right) + N\Delta((g_2 + 4\tilde{g}_2 A) + 6g_4\Delta), \quad (5.4)$$

where Δ is determined by the quadratic equation

$$12g_4\Delta^2 + (g_2 + 4\tilde{g}_2 A)\Delta = S. \quad (5.5)$$

Now we can integrate A out and obtain the superpotential for the glueball superfield S . We solve $\partial W_{\text{eff}}/\partial A = \partial W_{\text{single}}/\partial A - 2\tilde{g}_2 A = 0$ for A . This is a simple calculation from (5.4), (5.5):

$$\begin{aligned} \frac{\partial}{\partial A} W_{\text{single}}(\Delta(S, A), S, A) &= \frac{\partial W_{\text{single}}}{\partial A} + \frac{\partial \Delta}{\partial A} \frac{\partial W_{\text{single}}}{\partial \Delta} \\ &= (g_2 + 4\tilde{g}_2 A + 12g_4\Delta - \frac{S}{\Delta})N \frac{\partial \Delta}{\partial A} + 4\tilde{g}_2 N\Delta \\ &= 4\tilde{g}_2 2N\Delta, \end{aligned} \quad (5.6)$$

where in last step we have used (5.5). So the solution to $\partial W_{\text{single}}/\partial A - 2\tilde{g}_2 A = 0$ is

$$A = 2N\Delta. \quad (5.7)$$

Plugging $A = 2N\Delta$ into (5.4), (5.5) and (5.3), we find the effective glueball superpotential to be

$$W_{\text{eff}} = NS \log\left(\frac{\Lambda^2}{\Delta}\right) + N\Delta(g_2 + 4\tilde{g}_2 N\Delta + 6g_4\Delta), \quad (5.8)$$

with Δ determined by the quadratic equation

$$(12g_4 + 8\tilde{g}_2 N)\Delta^2 + g_2\Delta = S. \quad (5.9)$$

Equations (5.8) and (5.9) are of course the double-trace effective glueball superpotential we computed previously in (3.29) and (3.30).

Why does this procedure reproduce precisely the sum of pasted diagrams that contribute to the double-trace superpotential in (2.39)? From the point of view of perturbation theory, we are doing the following. If we treat A as a constant, we should simply sum the planar diagrams in the

theory with a quartic superpotential, and after doing so, we obtain the superpotential $\int d^4x d^2\theta W$ with

$$W = W_{\text{connected planar}}(S, g_2 + 4\tilde{g}_2 A, g_4) - \tilde{g}_2 A^2. \quad (5.10)$$

Next, we should integrate out A . To do so, we write $A = A_0 + \tilde{A}$, where A_0 solves $\partial W/\partial A = 0$. We see that W becomes

$$W = W_{\text{connected planar}}(S, g_2 + 4\tilde{g}_2 A_0, g_4) - \tilde{g}_2 A_0^2 + c_2 \tilde{A}^2 + c_3 \tilde{A}^3 + \dots \quad (5.11)$$

What is the meaning of integrating over \tilde{A} ? From the diagrammatic point of view, \tilde{A} is the field that allows momentum to flow through the \tilde{g}_2 vertices. All diagrams where such momentum flow is prohibited are taken into account by the background value A_0 . Thus, picking A_0 takes the pasting process into account, whereas the further integrals over \tilde{A} should correspond to pinching diagrams. We already know that these latter diagrams should vanish from our diagrammatic analysis, and therefore we should simply drop all terms involving \tilde{A} . The final answer for W is thus

$$W = W_{\text{connected planar}}(S, g_2 + 4\tilde{g}_2 A_0, g_4) - \tilde{g}_2 A_0^2. \quad (5.12)$$

One can also see directly that integrating out \tilde{A} gives no contribution to the superpotential. In the diagrams that one can write down, there will be many loops of \tilde{A} , but there are no vertices that can absorb any fermionic momentum, and therefore these diagrams do not yield any contribution to the superpotential.

It is an interesting exercise to verify explicitly that (5.12) is a generating diagram for pasted diagrams (which are all tree graphs), made out of building blocks corresponding to $W_{\text{connected planar}}$.

5.2 Matrix model perspective

Above we argued that the methods of [4] show that above linearization of the double-trace deformation via introduction of an auxiliary singlet field A leads to a theory whose superpotential be computed by a matrix model.

First observe that the double-trace matrix model partition function can be linearized in traces by the introduction of an auxiliary parameter A , over which we integrate:

$$\begin{aligned} Z = \exp(-M^2 \mathcal{F}_0^{\text{double}}) &= \int d^{M^2}(\Phi) \exp\left\{-M\left(\frac{1}{2}g_2 \text{Tr}(\Phi^2) + g_4 \text{Tr}(\Phi^4) + \tilde{g}_2 \frac{(\text{Tr}(\Phi^2))^2}{M}\right)\right\} \\ &= \int dA d^{M^2}(\Phi) \exp\left\{-M\left(\frac{1}{2}(g_2 + 4\tilde{g}_2 A) \text{Tr}(\Phi^2) + g_4 \text{Tr}(\Phi^4) - M\tilde{g}_2 A^2\right)\right\}. \end{aligned} \quad (5.13)$$

This is Matrix model analog of the statement that the double-trace field theory can be generated by integrating out a gauge singlet. In terms of the free energy of the single-trace matrix model, this can be written as

$$\exp(-M^2 \mathcal{F}_0^{\text{double}}) = \int dA \exp(-M^2 \mathcal{F}_0^{\text{single}} + M^2 \tilde{g}_2 A^2). \quad (5.14)$$

Hence to obtain the free energy of the double-trace matrix model, we need to solve the equation $\frac{\partial \mathcal{F}_0^{\text{single}}(A, S)}{\partial A} - 2\tilde{g}_2 A = 0$ for A and substitute in $\mathcal{F}_0^{\text{double}} = \mathcal{F}_0^{\text{single}}(A, S) - \tilde{g}_2 A^2$ where we have

used the identification from [3] that $S \sim M$. The resulting expression for the double-trace matrix model is, of course, the same as that obtained by mean field methods in section (4.1). However, as emphasized in the previous sections, the derivative of this free energy with respect to S does *not* yield the correct superpotential for the field theory.

Let us now contrast this with a *different* matrix model construction suggested by the field theory analysis in the previous subsection. Consider the Matrix partition function

$$\tilde{Z} = \exp(-M^2 \mathcal{F}_0^{\text{single}}) = \int d^{M^2}(\Phi) \exp\{-M(\frac{1}{2}(g_2 + 4\tilde{g}_2 A)\text{Tr}(\Phi^2) + g_4 \text{Tr}(\Phi^4))\}, \quad (5.15)$$

where A is now treated as a fixed parameter of the Matrix model in analogy with the constant A appearing in the field theory superpotential. As we explained above, the arguments of [4] applied to the linearized model (5.2) show that in terms of $\mathcal{F}_0^{\text{single}}(A, S)$ (with $S \sim M$ as in [3])

$$W_{\text{eff}}(A, S) = -NS(\log(S/\Lambda^2) - 1) + N \frac{\partial \mathcal{F}_0^{\text{single}}}{\partial S} \Bigg|_{\text{constant } A} - \tilde{g}_2 A^2, \quad (5.16)$$

where W_{eff} is the field theory superpotential in (5.3). Note that we have *not* integrated out A at this stage. Since the single-trace matrix model has reproduced $W_{\text{eff}}(A, S)$, it is manifest that integrating out A will correctly produce the double-trace superpotential as a function of the glueball, just as it did in the field theory.

Identifying the glueball: Something remarkable appears to have happened here. If we start with the single-trace Matrix model (5.13) and integrate out the singlet A , we find the free energy of the double-trace model as indicated in (5.14), and $\partial \mathcal{F}_0^{\text{double}}/\partial S$ does not reproduce the field theory superpotential. However, if we first differentiate with respect to S and *then* integrate out A we reproduce the field theory result. Of course, the direct field theory computation described above indicates to us that this is the right order in which to do things. But notice that the difference between the two procedures essentially amounts to correctly identifying the glueball. Apparently to identify S in the Matrix model we must linearize the theory and then use the prescription given in [3]. Of course, differentiating the single-trace free energy with respect to S at constant A translates in the double-trace theory into some complicated operation which would in effect identify the field theory glueball in that Matrix model. But it is challenging to identify what this operation is.

5.3 General Multi-trace Operators

Finally, we show that the procedure of introducing auxiliary parameters to linearize traces in a double-trace theory can be extended to a general multi-trace model. Consider the term

$$\text{Tr}(\Phi^{m_1})\text{Tr}(\Phi^{m_2}). \quad (5.17)$$

in the superpotential. We can rewrite this in terms of single trace terms by introducing four gauge singlet fields A_i , $i = 1 \cdots 4$ as

$$W_2 = 3\left(A_1^2 + A_2^2 + A_1 A_2 + A_1 \text{Tr} \Phi^{m_1} + A_2 \text{Tr}(\Phi^{m_2} + \frac{2}{\sqrt{3}} A_3 \text{Tr} \Phi^{m_1} - A_3^2 + \frac{2}{\sqrt{3}} A_4 \text{Tr} \Phi^{m_2} - A_4^2)\right). \quad (5.18)$$

Integrating out A_i by setting $\partial W_2/\partial A_i = 0$, solving for A_i and substituting in (5.18) yields the double trace superpotential (5.17).

To generate a term of the form

$$\mathrm{Tr}(\Phi^{m_1})\mathrm{Tr}(\Phi^{m_2})\mathrm{Tr}(\Phi^{m_3}) . \quad (5.19)$$

we iterate the above procedure twice, *i.e.* we introduce additional gauge singlet fields B_i , $i = 1 \cdots 4$, and consider the theory with a superpotential

$$W_3 = 3\left(B_1^2 + B_2^2 + B_1 B_2 + B_1 \mathrm{Tr} \Phi^{m_3} + B_2 W_2 + \frac{2}{\sqrt{3}} B_3 \mathrm{Tr} \Phi^{m_3} - B_3^2 + \frac{2}{\sqrt{3}} B_4 W_2 - B_4^2\right). \quad (5.20)$$

where W_2 is defined in (5.18). Integrating out A_i and B_i for $i = 1 \cdots 4$ yields the term (5.19). Generalization to terms with more traces is obvious.

6. Conclusion

We have studied an $\mathcal{N} = 1$ $U(N)$ gauge theory with adjoint chiral matter and a double-trace tree-level superpotential. We found by direct computation that the computation of the effective superpotential as a function of the glueball superfield localizes to summing a set of matrix integrals. The associated set of Matrix diagrams have the structure of tree diagrams in which double-trace vertices are strung together by “propagators” and “external” legs are that themselves connected single-trace diagrams. We showed that the Seiberg-Witten solution to $\mathcal{N} = 2$ field theories computes an effective superpotential for the double-trace theory that matches our direct analysis. The use of factorization in our Seiberg-Witten analysis, namely that $\langle \mathrm{Tr}(\Phi^2)^2 \rangle = \langle \mathrm{Tr}(\Phi^2) \rangle^2$, was equivalent in our perturbative computations to the vanishing of any diagrams where extra momentum loops were introduced by the double-trace vertices. Next, we showed that the large- M limit of the standard double-trace $U(M)$ Matrix model does sum up the same set of matrix diagrams, but the combinatorial factors are different from those appearing in the field theory. In particular, the field theory superpotential is not computed by a derivative of the matrix model free energy as in [3]. Put another way, a simple manipulation of the free energy of the standard double-trace matrix model does not give a generating function for the field theory superpotential. Finally we demonstrated how a multi-trace field theory can be linearized in traces by the introduction of auxiliary singlet fields. We showed the associated Matrix model, which is linear in traces also, computes the field theory superpotential as a function of both the glueball and the new singlets. The basic subtlety, then, lies in the correct identification of the field theory glueball as a variable in a Matrix model.

Our results raise several challenges:

1. We found that while a multi-trace Matrix model did not directly compute the superpotential of a multi-trace field theory, we could sum the necessary diagrams by introducing auxiliary singlet fields in an associated single-trace model. The basic subtlety involves correct identification of the field theory glueball in the Matrix model. How is this done in general, and what is the underlying principle driving the identification?

2. Does the large- N limit of the standard double-trace Matrix model compute the superpotential for some $\mathcal{N} = 1$ field theory?
3. We expect that all our results generalize easily to multi-trace theories — it would be nice to check this.
4. We have worked in the vacuum with an unbroken gauge group. It would be good to generalize our arguments to the other vacua with partially broken gauge symmetry.
5. In Sec. 2.6 we pointed out that there is an intriguing connection between the contributions made by multi-trace vertices to the superpotential of a local theory and certain Feynman diagrams of an associated *nonlocal* theory. It would be very interesting to flesh out this connection.
6. In an $U(N)$ theory with adjoint Φ , the operator $\text{Tr}(\Phi^K)$ with $K > N$ decomposes into a sum of multi-trace operators. This decomposition can receive quantum corrections as discussed in [5]. How do our arguments generalize to this case?
7. We can also add baryon-like operators like $\det(\Phi)$ to the superpotential (for theories with fundamental matter in the context of matrix models, baryons were studied by [16, 17]). Such operators also decompose into sums of products of traces, and are very interesting because, even without fundamental matter, they can give rise to an *open* string sector in Yang-Mills theory as opposed to the standard closed string sector that the 't Hooft expansion leads us to expect [37, 38]. It would be useful to understand in this case how and whether the computation of holomorphic data in such a theory localizes to sums of Matrix integrals.

In addition to these directions there are some interesting applications that arise from known facts about the large- N of the standard double-trace $U(N)$ Matrix model. This theory is related to two-dimensional gravity with a positive cosmological constant and displays phase transitions between branched polymer and smooth phases of two-dimensional gravity [22]. Presumably such phase transitions manifest themselves as interesting phenomena in a four-dimensional field theory.

Acknowledgments

Work on this project at the University of Pennsylvania was supported by the DOE under cooperative research agreement DE-FG02-95ER40893, and by an NSF Focused Research Grant DMS0139799 for “The Geometry of Superstrings”. This research was also supported by the Institute for Advanced Study, under the NSF grant PHY-0070928 and the Virginia Polytechnic Institute and State University, under the DOE grant DE-FG05-92ER40709. We gratefully acknowledge J. Erlich for participation in the earlier stages of the work and D. Berenstein, P. Berglund, F. Cachazo, R. Dijkgraaf, A. Hanany, K. Intriligator, P. Kraus, R. Leigh, M. Mariño, D. Minic, J. McGreevy, N. Seiberg, and C. Vafa for comments and revelations. We thank Ravi Nicholas Balasubramanian for inspirational babbling. BF and VJ also express their appreciation of the most generous hospitality of the

High Energy Group at the University of Pennsylvania; they and YHH further toast to W. Buchanan of La Reserve B & B for his warm congeniality.

References

- [1] R. Dijkgraaf and C. Vafa, ‘*Matrix models, topological strings, and supersymmetric gauge theories,*’ *Nucl. Phys.* **B644** (2002) 3–20, <http://arXiv.org/abs/hep-th/0206255>.
- [2] R. Dijkgraaf and C. Vafa, ‘*On geometry and matrix models,*’ *Nucl. Phys.* **B644** (2002) 21–39, <http://arXiv.org/abs/hep-th/0207106>.
- [3] R. Dijkgraaf and C. Vafa, ‘*A perturbative window into non-perturbative physics,*’ <http://arXiv.org/abs/hep-th/0208048>.
- [4] R. Dijkgraaf, M. T. Grisaru, C. S. Lam, C. Vafa, and D. Zanon, ‘*Perturbative computation of glueball superpotentials,*’ <http://arXiv.org/abs/hep-th/0211017>.
- [5] F. Cachazo, M. R. Douglas, N. Seiberg and E. Witten, “Chiral Rings and Anomalies in Supersymmetric Gauge Theory,” [arXiv:hep-th/0211170](http://arXiv.org/abs/hep-th/0211170).
- [6] N. Dorey, T. J. Hollowood, S. P. Kumar and A. Sinkovics, “Massive vacua of $N = 1^*$ theory and S-duality from matrix models,” [arXiv:hep-th/0209099](http://arXiv.org/abs/hep-th/0209099).
- [7] N. Dorey, T. J. Hollowood, S. Prem Kumar and A. Sinkovics, “Exact superpotentials from matrix models,” [arXiv:hep-th/0209089](http://arXiv.org/abs/hep-th/0209089).
- [8] R. Argurio, V. L. Campos, G. Ferretti and R. Heise, “Exact superpotentials for theories with flavors via a matrix integral,” [arXiv:hep-th/0210291](http://arXiv.org/abs/hep-th/0210291).
- [9] J. McGreevy, “Adding flavor to Dijkgraaf-Vafa,” [hep-th/0211009](http://arXiv.org/abs/hep-th/0211009).
- [10] D. Berenstein, “Quantum moduli spaces from matrix models,” [arXiv:hep-th/0210183](http://arXiv.org/abs/hep-th/0210183).
- [11] R. Dijkgraaf, A. Neitzke and C. Vafa, “Large N Strong Coupling Dynamics in Non-Supersymmetric Orbifold Field Theories,” [arXiv:hep-th/0211194](http://arXiv.org/abs/hep-th/0211194).
- [12] H. Ita, H. Nieder and Y. Oz, “Perturbative computation of glueball superpotentials for $SO(N)$ and $USp(N)$,” [arXiv:hep-th/0211261](http://arXiv.org/abs/hep-th/0211261).
- [13] R. A. Janik and N. A. Obers, “ $SO(N)$ Superpotential, Seiberg-Witten Curves and Loop Equations,” [arXiv:hep-th/0212069](http://arXiv.org/abs/hep-th/0212069).
- [14] S. K. Ashok, R. Corrado, N. Halmagyi, K. D. Kennaway and C. Romelsberger, “Unoriented Strings, Loop Equations, and $N=1$ Superpotentials from Matrix Models,” [arXiv:hep-th/0211291](http://arXiv.org/abs/hep-th/0211291).
- [15] B. Feng, “Geometric Dual and Matrix Theory for SO/Sp Gauge Theories,” [hep-th/0212010](http://arXiv.org/abs/hep-th/0212010).
- [16] R. Argurio, V. L. Campos, G. Ferretti and R. Heise, “Baryonic Corrections to Superpotentials from Perturbation Theory,” [arXiv:hep-th/0211249](http://arXiv.org/abs/hep-th/0211249).
- [17] I. Bena, R. Roiban and R. Tatar, “Baryons, Boundaries and Matrix Models,” [arXiv:hep-th/0211271](http://arXiv.org/abs/hep-th/0211271).
- [18] A. Klemm, M. Marino and S. Theisen, “Gravitational corrections in supersymmetric gauge theory and matrix models,” [arXiv:hep-th/0211216](http://arXiv.org/abs/hep-th/0211216).

- [19] R. Dijkgraaf, A. Sinkovics and M. Temurhan, “Matrix Models and Gravitational Corrections,” arXiv:hep-th/0211241.
- [20] B. Feng, “Seiberg Duality in Matrix Model,” arXiv:hep-th/0211202.
- [21] B. Feng and Y. H. He, “Seiberg Duality in Matrix Models II,” arXiv:hep-th/0211234.
- [22] S. R. Das, A. Dhar, A. M. Sengupta, and S. R. Wadia, ‘*New critical behavior in $d = 0$ large N matrix models,*’ *Mod. Phys. Lett.* **A5** (1990) 1041–1056.
- [23] D. Berenstein, ‘*Reverse geometric engineering of singularities,*’ *JHEP* **04** (2002) 052, <http://arXiv.org/abs/hep-th/0201093>.
- [24] O. Aharony, M. Berkooz and E. Silverstein, “Multiple-Trace Operators and Non-Local String Theories,” hep-th/0105309.
- [25] G. Veneziano and S. Yankielowicz, “An Effective Lagrangian For The Pure $N=1$ Supersymmetric Yang-Mills Theory,” *Phys. Lett. B* **113**, 231 (1982).
- [26] E. Brezin, C. Itzykson, G. Parisi, and J. B. Zuber, ‘*Planar Diagrams,*’ *Commun. Math. Phys.* **59** (1978) 35.
- [27] N. Seiberg, E. Witten, “Monopole Condensation, And Confinement In $N=2$ Supersymmetric Yang-Mills Theory,” hep-th/9407087;
“Monopoles, Duality and Chiral Symmetry Breaking in $N=2$ Supersymmetric QCD,” hep-th/9408099.
- [28] F. Cachazo, K. A. Intriligator, and C. Vafa, ‘*A large N duality via a geometric transition,*’ *Nucl. Phys.* **B603** (2001) 3–41, <http://arXiv.org/abs/hep-th/0103067>.
- [29] F. Ferrari, “On exact superpotentials in confining vacua,” arXiv:hep-th/0210135.
- [30] F. Cachazo and C. Vafa, ‘ *$N = 1$ and $N = 2$ geometry from fluxes,*’ <http://arXiv.org/abs/hep-th/0206017>.
- [31] K. Intriligator, “Integrating in and exact superpotentials in 4d,” hep-th/9407106.
- [32] M. Douglas, S. Shenker, “Dynamics of $SU(N)$ Supersymmetric Gauge Theory,” hep-th/9503163.
- [33] I. R. Klebanov and A. Hashimoto, ‘*Nonperturbative solution of matrix models modified by trace squared terms,*’ *Nucl. Phys.* **B434** (1995) 264–282, <http://arXiv.org/abs/hep-th/9409064>;
- [34] S. S. Gubser and I. Mitra, “Double-trace operators and one-loop vacuum energy in AdS/CFT,” arXiv:hep-th/0210093.
- [35] R. Dijkgraaf, S. Gukov, V. A. Kazakov and C. Vafa, “Perturbative analysis of gauged matrix models,” arXiv:hep-th/0210238.
- [36] A. V. Bitsadze, ‘*Integral Equations of First Kind,*’,
T. Carleman, ‘*Über die Abelsche Integralgleichung mit Konstanten Integrationsgrenzen,*’ *Mathematische Zeitschrift* **15** (1922) 111–120.
- [37] V. Balasubramanian, M. x. Huang, T. S. Levi and A. Naqvi, “Open strings from $N = 4$ super Yang-Mills,” *JHEP* **0208**, 037 (2002) [arXiv:hep-th/0204196].
- [38] O. Aharony, Y. E. Antebi, M. Berkooz and R. Fishman, “‘Holey sheets’: Pfaffians and subdeterminants as D-brane operators in large N gauge theories,” arXiv:hep-th/0211152.